Event plane dependence of di-hadron correlations with event shape engineering at the STAR experiment

Ryo Aoyama, for the STAR collaboration
University of Tsukuba, TCHoU
May 15th, 2018
Quark Matter 2018 @Venezia

Jets with di-hadron correlations in high energy nuclear collisions

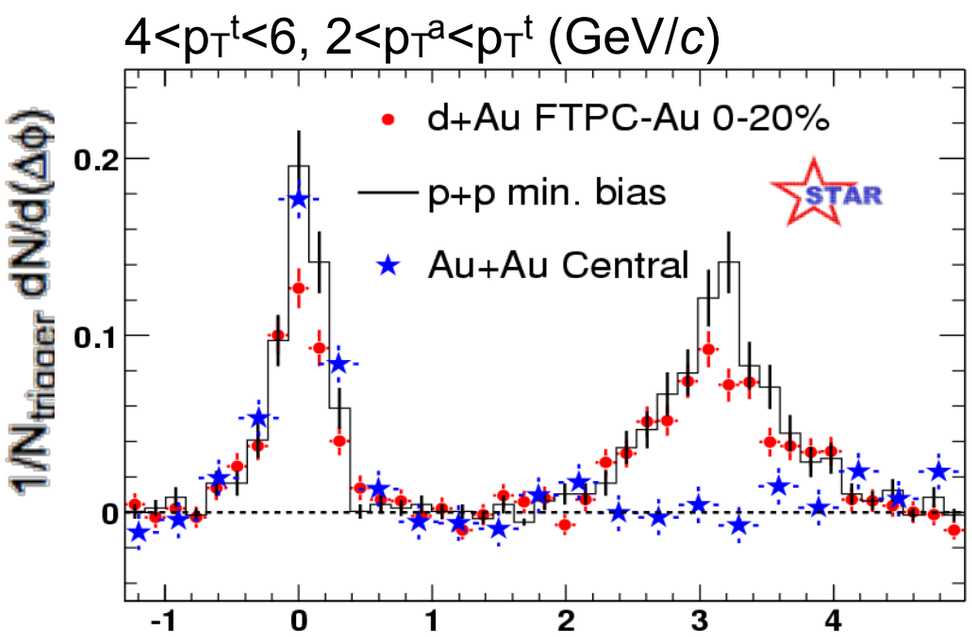

STAR, PRL 91, 072304 (2003) Δ φ (radians)

only v_2 subtraction applied

PHENIX, PRC 78, 014901 (2008)

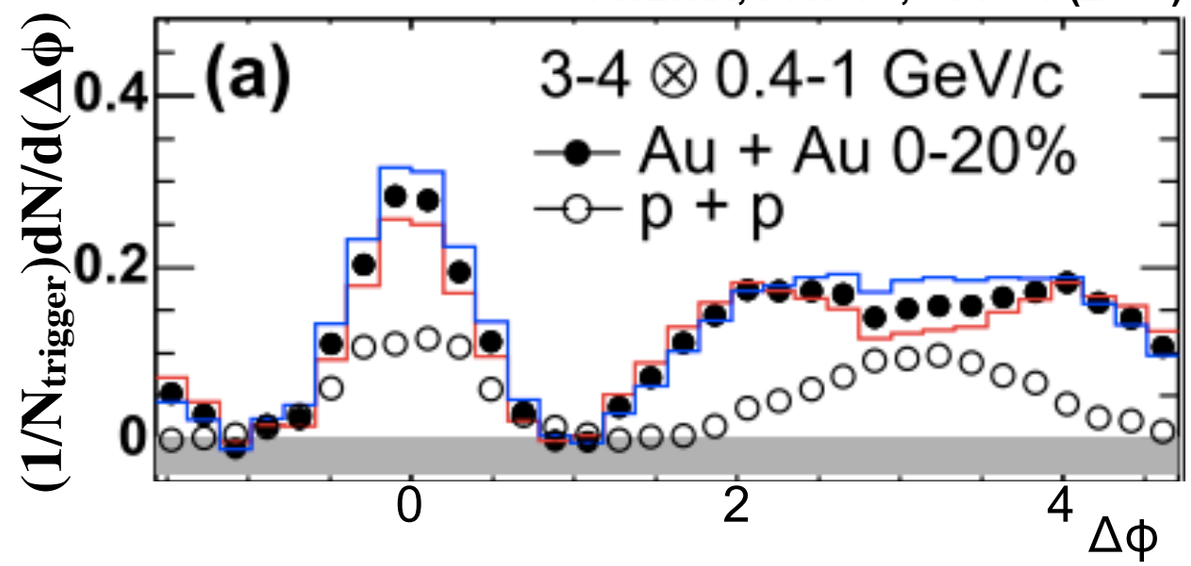

only v_2 subtraction applied

Hard scattering of partons ➡ back-to-back jets

Jets probe energy loss mechanisms in the QGP

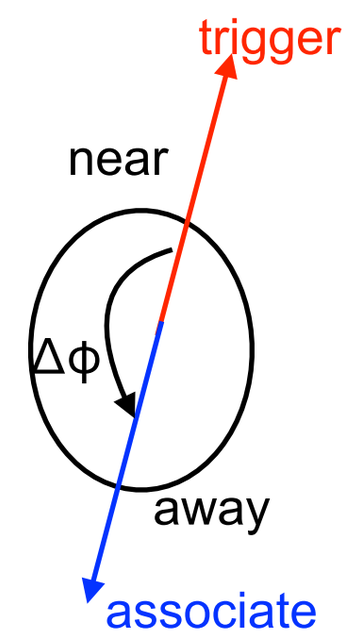

- ✦ Strong suppression of high-p_T particles in back-to-back direction
  - partonic energy loss
- ✦ Low-p_T particles are enhanced at large angles
  - softening and broadening

➡ Probe path-length dependence with a more differential measurement

Event plane and higher order flow harmonics

- Spatial anisotropy due to **almond-like shape** and **event-by-event fluctuations** of overlapping region of nuclei in non-central heavy-ion collisions
- Deformation converted into momentum space by **collective motion** (**flow**)
  - azimuthal anisotropy

azimuthal distribution : $\frac{dN}{d\phi} \propto 1 + \sum_i 2v_n \cos n(\phi - \Psi_n)$

n-th order event plane : $\Psi_n = \frac{1}{n} \cdot \frac{\sum w_i \sin(n\phi_i)}{\sum w_i \cos(n\phi_i)}$

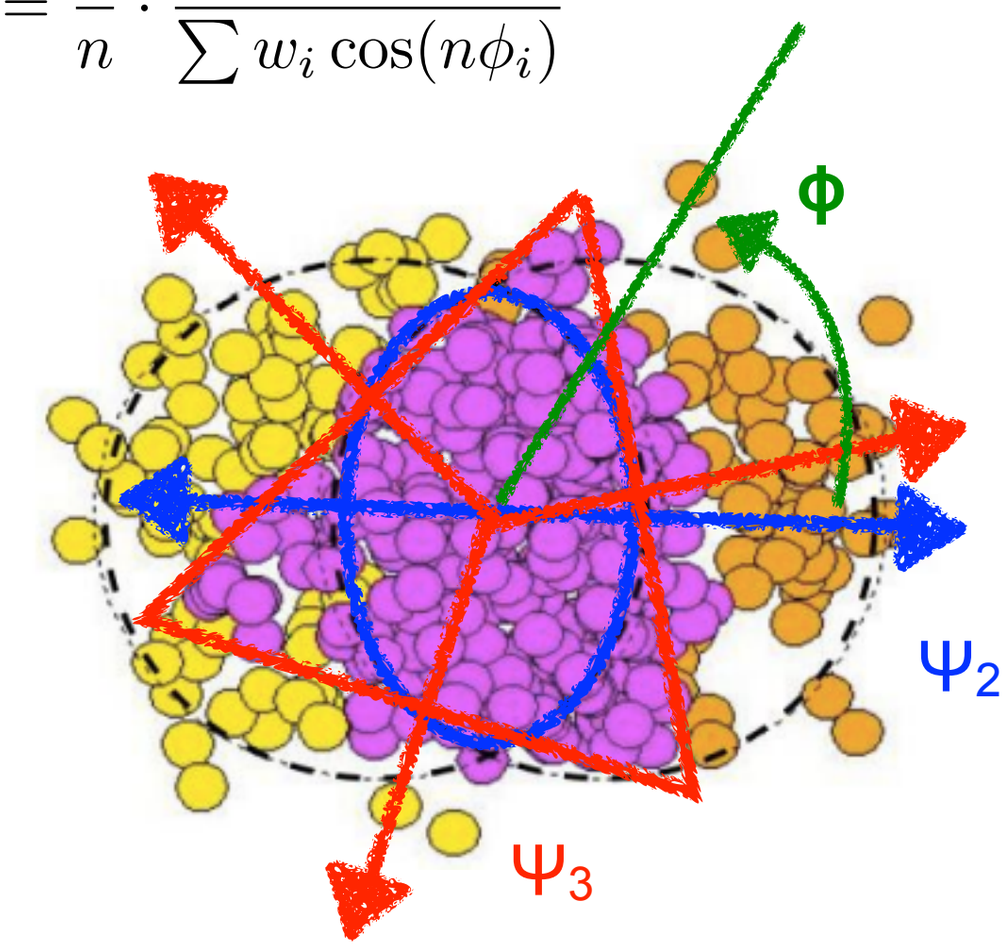

Event plane dependent di-hadron correlations

ϕ_s : trigger angle with respect to event plane ($=\phi-\Psi_2$)

STAR, PRC 89, 041901 (2014)

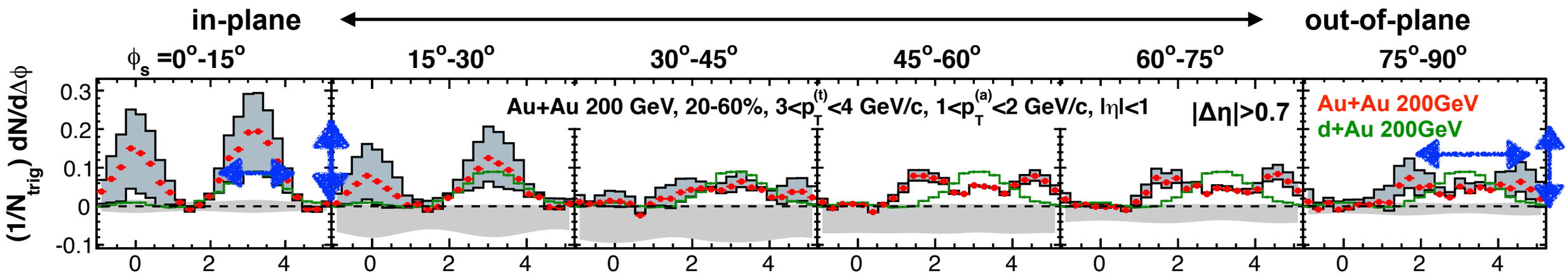

v_2, v_3, v_4 subtracted

$\Delta\phi=\phi_{asso}-\phi_{trig}$

No ESE

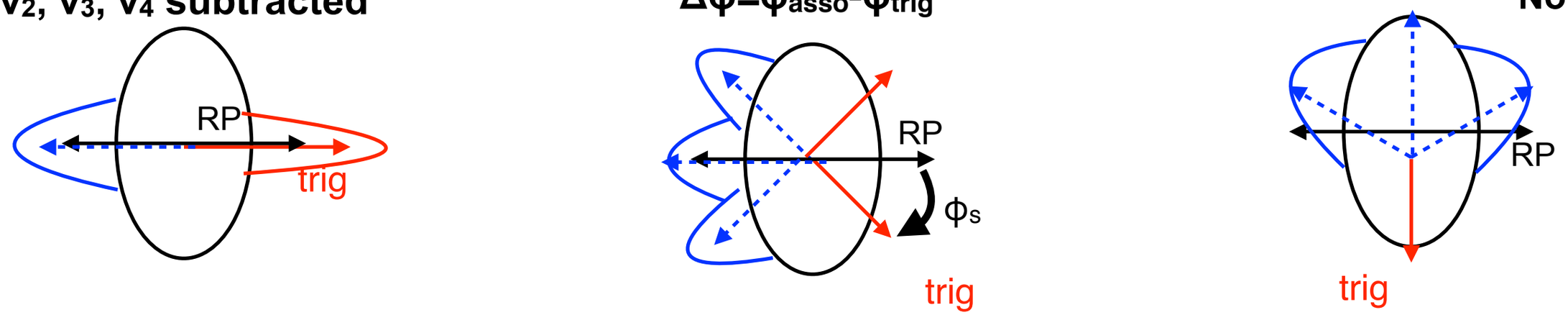

- EP-dependent long-range correlation (ridge) measurement
- Implication of path-length dependence of energy loss
  - Away-side peak becomes lower and broadened as trigger direction changes from in-plane to out-of-plane
    - **Path-length dependent enhancement of yield**

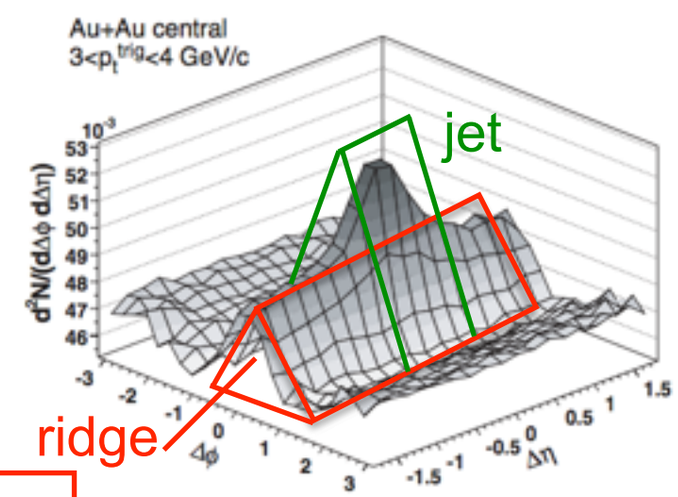

STAR, PRC 80, 064912 (2009)

Rest of this talk : **|Δη|<1** ► jet cone AND away-side are focused on

Event shape engineering (ESE)

- Possibility to control the initial eccentricity
  - Event-by-event v_2 amplitude is selected by the magnitude of flow vector q_2

$$Q_{2,x} = \sum w_i \cos(2\phi_i)$$
$$Q_{2,y} = \sum w_i \sin(2\phi_i)$$
$$q_2 = \sqrt{Q_{2,x}^2 + Q_{2,y}^2} / \sqrt{\sum w_i}$$

w_i : weighting factor

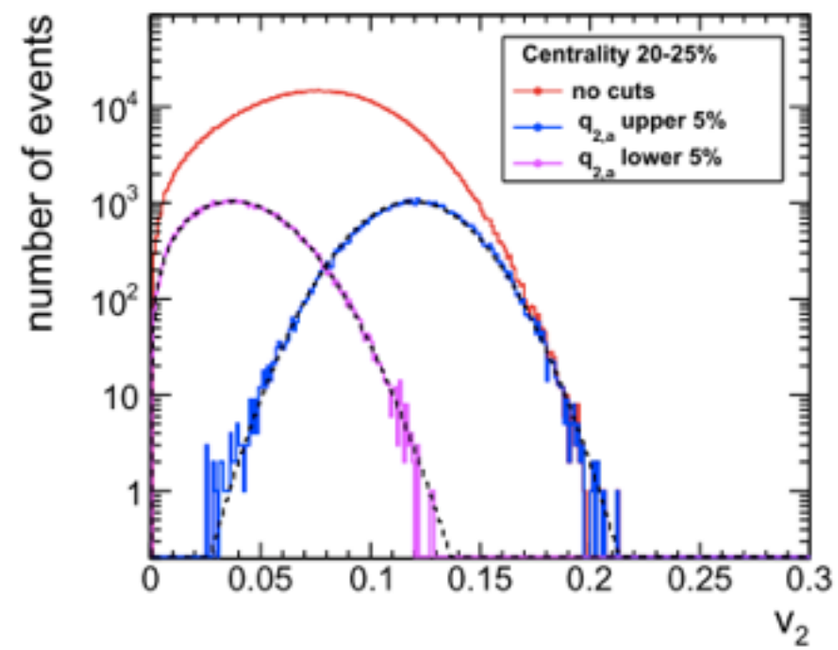

correlation between q_2 and ε_2

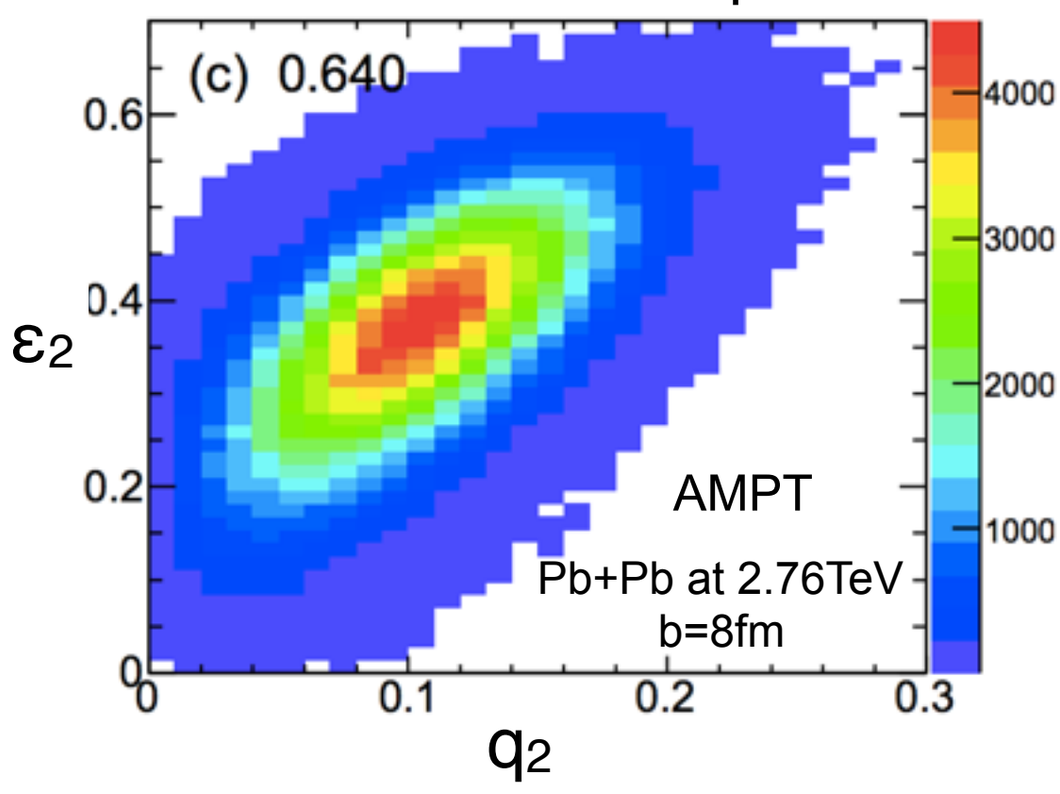

- v_2 fluctuates in a given centrality bin
- q_2 can bias towards event-by-event v_2
- ε_2 is correlated with q_2

initial eccentricity $\varepsilon_2 = \frac{\langle x^2 - y^2 \rangle}{\langle x^2 + y^2 \rangle}$

J.Schukraft, A.Timmins and S.A.Voloshin, PLB 719 (2013), 394-398

A.M.Poskanzer, S.A.Voloshin, PRC 58 (1998), 1671-1678

J.Jia, P.Huo, PRC 90 (2014), 034915

Motivation

- Combination of centrality selection and event shape engineering allows control of the initial geometry while keeping the average energy density (multiplicity) fixed
  - Study difference in medium expansion
- Di-hadron correlations with event shape engineering allow new differential insight into energy loss mechanisms as a function of initial energy and shape
  - Detailed information which was previously averaged out

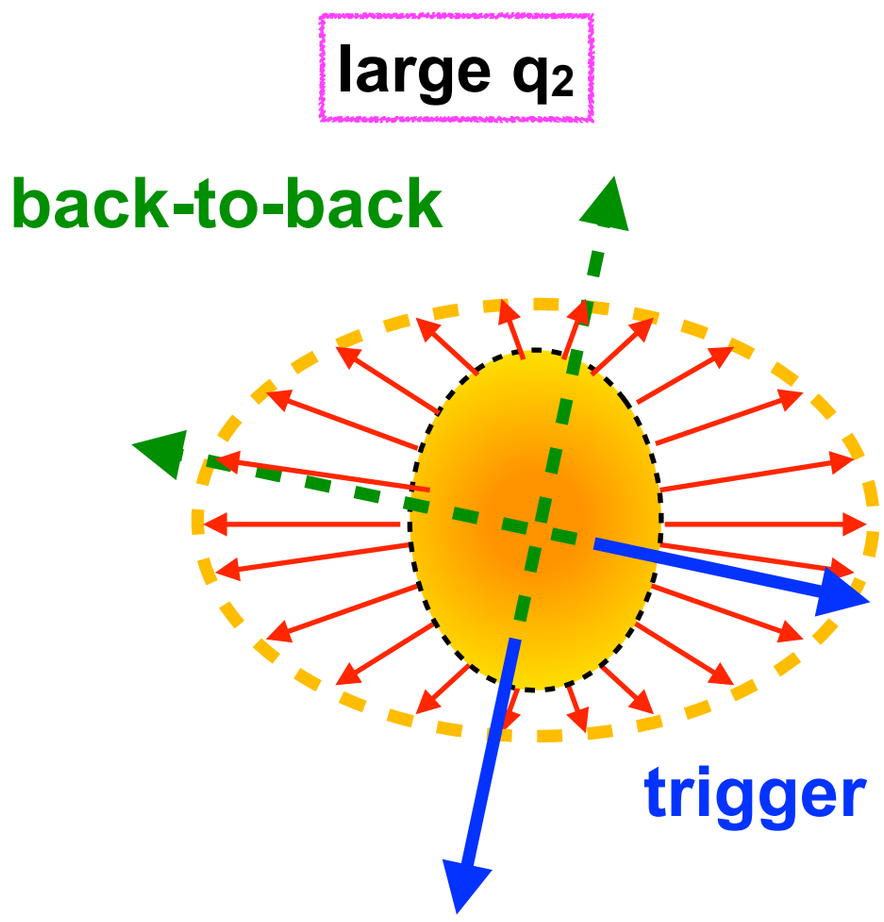

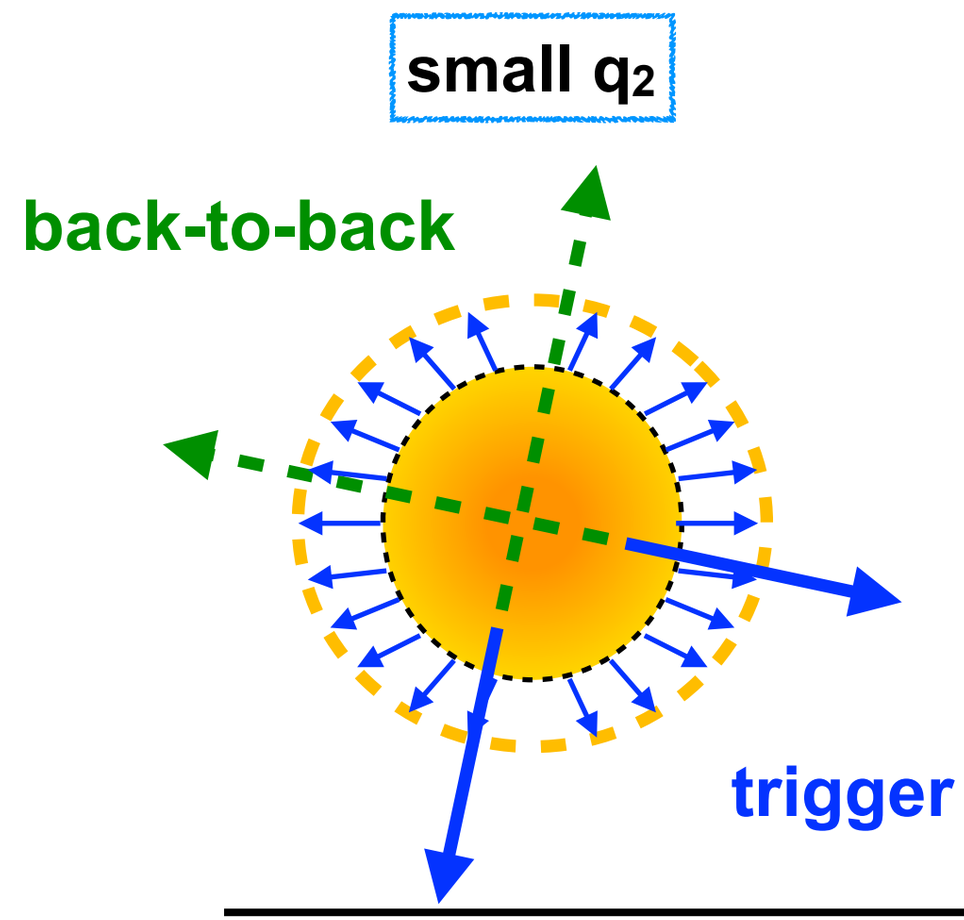

Data analysis

- **Data set**
  - **Minimum bias Au+Au at $\sqrt{s_{NN}}$ = 200 GeV collected by STAR in 2011**

Analysis

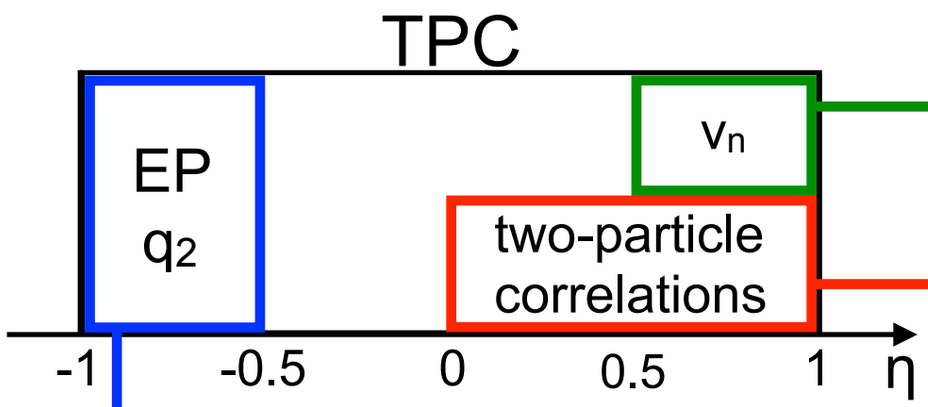

- **v_n measurement via EP method**
- **Two-particle correlations**

$$C(\Delta\phi) \propto \frac{N_{pair}^{real}(\Delta\phi)}{N_{pair}^{mix}(\Delta\phi)}$$

- **Event Plane Ψ_n**
- **q_2 selection**
  - top 20% and bottom 20%

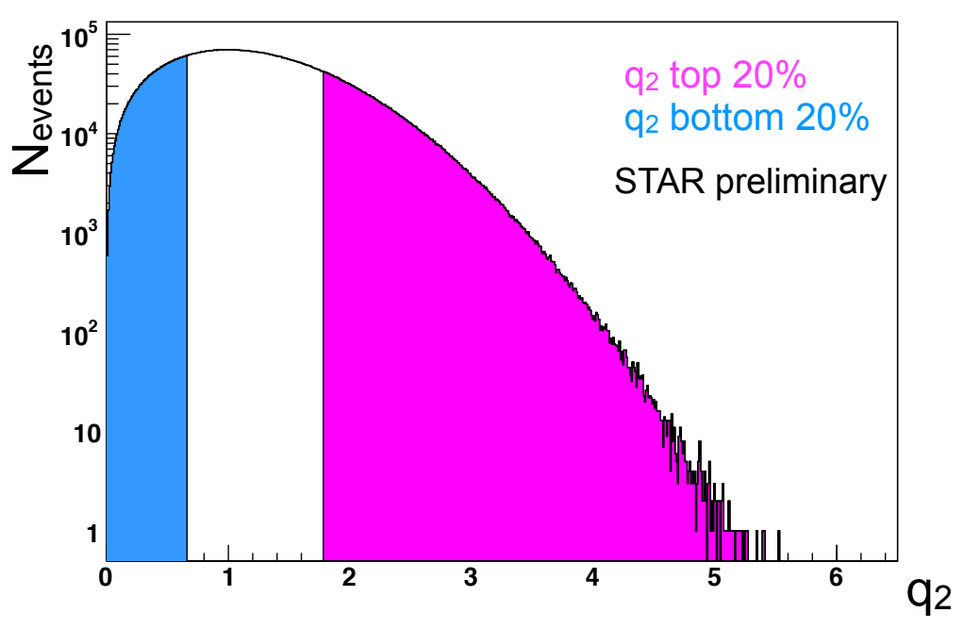

trigger angle selection w.r.t. EP

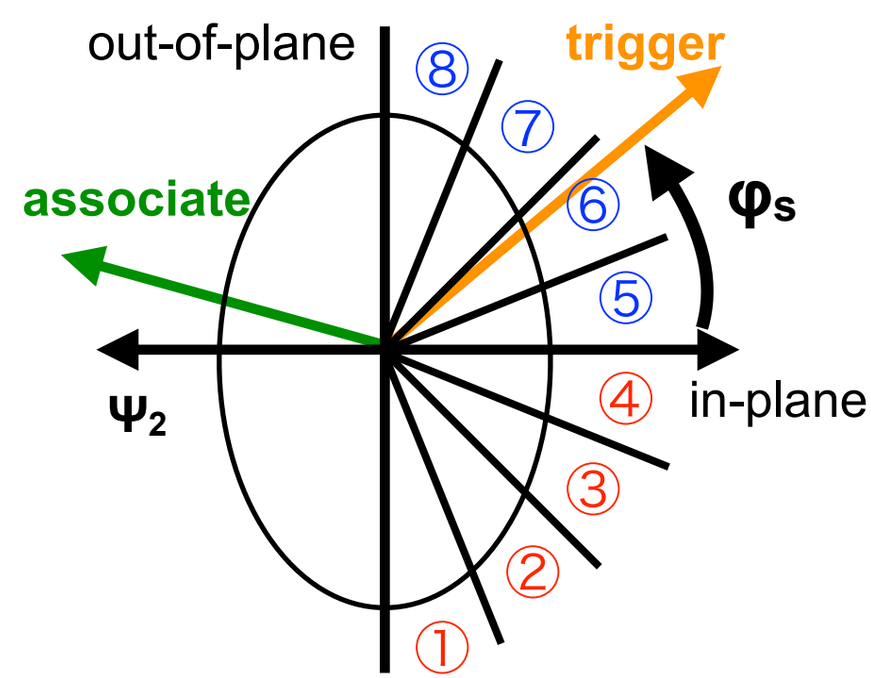

v_2 with ESE

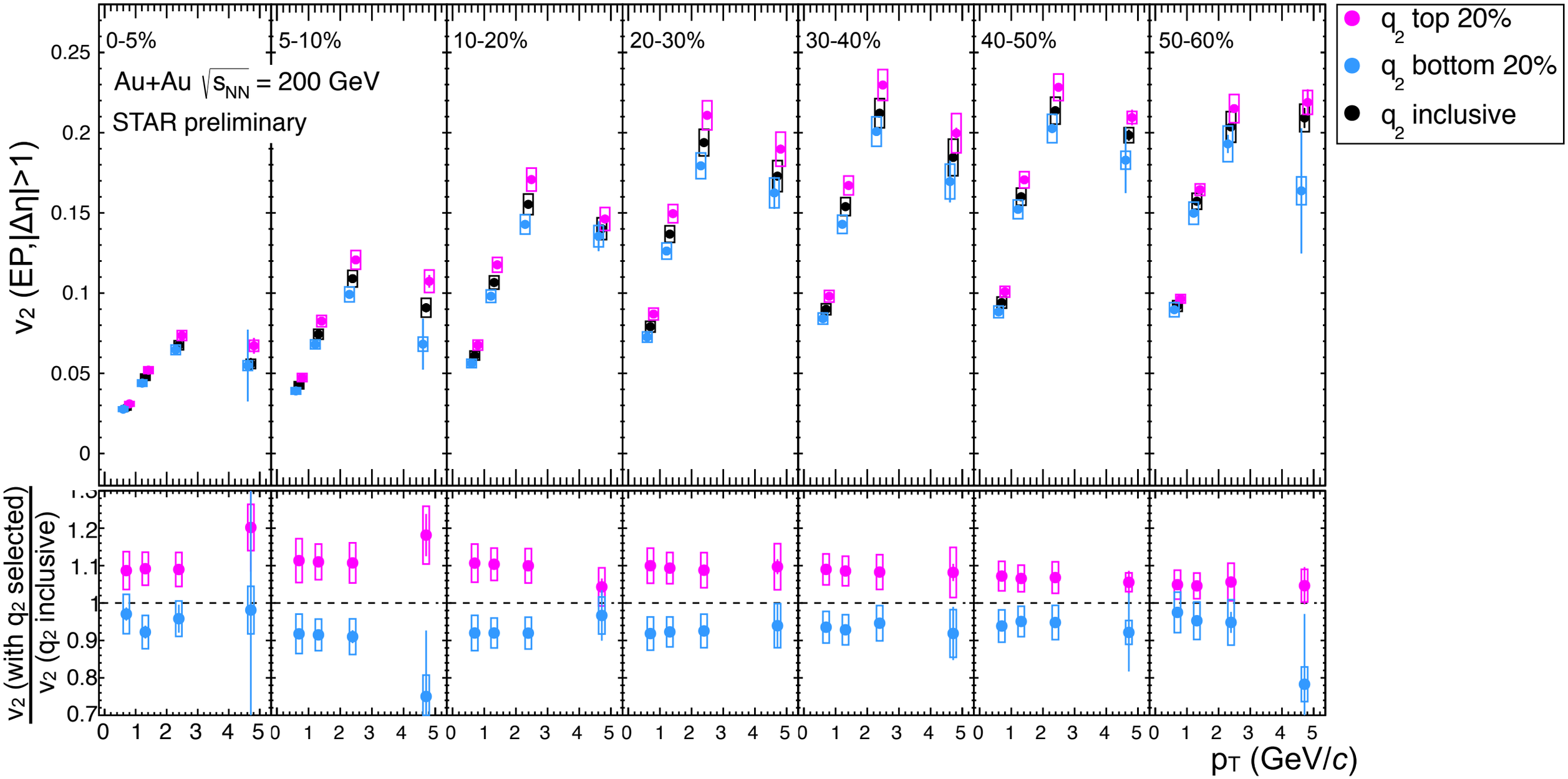

- ✦ v_2 is measured via event plane method with TPC-EP
- ✦ 20% largest and smallest q_2 vectors are selected with the same region as TPC-EP
- ✦ Top 20% q_2 selection leads to **~10% larger v_2 events**
- ✦ Bottom 20% q_2 selection leads to **~8% smaller v_2 events**

Correlations before flow subtraction and EP correction

Au+Au $\sqrt{s_{NN}}$ = 200 GeV
20-30%, w/o q_2 selection
$p_T^t \times p_T^a$=4-10x2-4 (GeV/*c*)

● raw data
— background function ($v_2 \oplus v_3 \oplus v_4$)

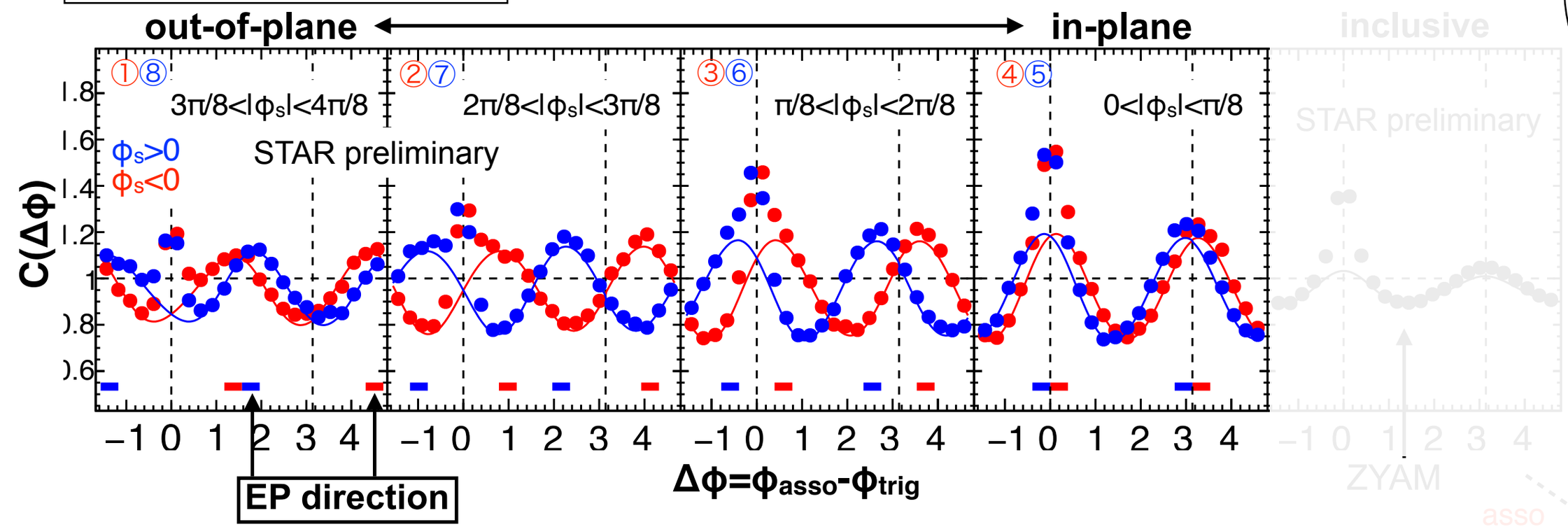

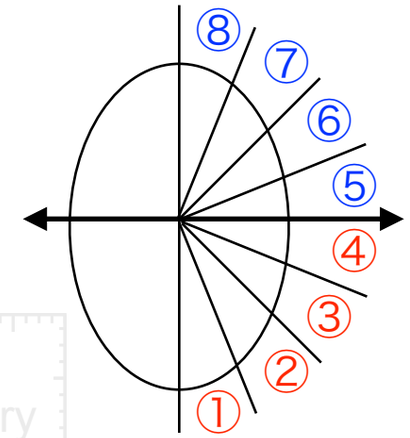

- ✦ Correlation shape
  - Left/Right mirror symmetric trigger selection w.r.t. EP leads to **mirror-imaged distributions** on the away side
- ✦ Flow background subtraction
  - Background **shape** is determined by data-driven simulation
  - Background **level** is determined by inclusive trigger data with ZYAM assumption
- ✦ Correction of trigger smearing effect
  - Smearing of trigger particle's angle due to limited EP resolution is corrected with unfolding method after flow subtraction

Correlations before flow subtraction and EP correction

Au+Au $\sqrt{s_{NN}}$ = 200 GeV
20-30%, w/o q_2 selection
$p_T^t \times p_T^a$=4-10x2-4 (GeV/*c*)

● raw data
— background function ($v_2 \oplus v_3 \oplus v_4$)

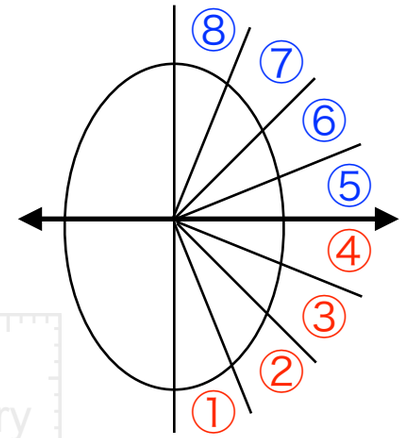

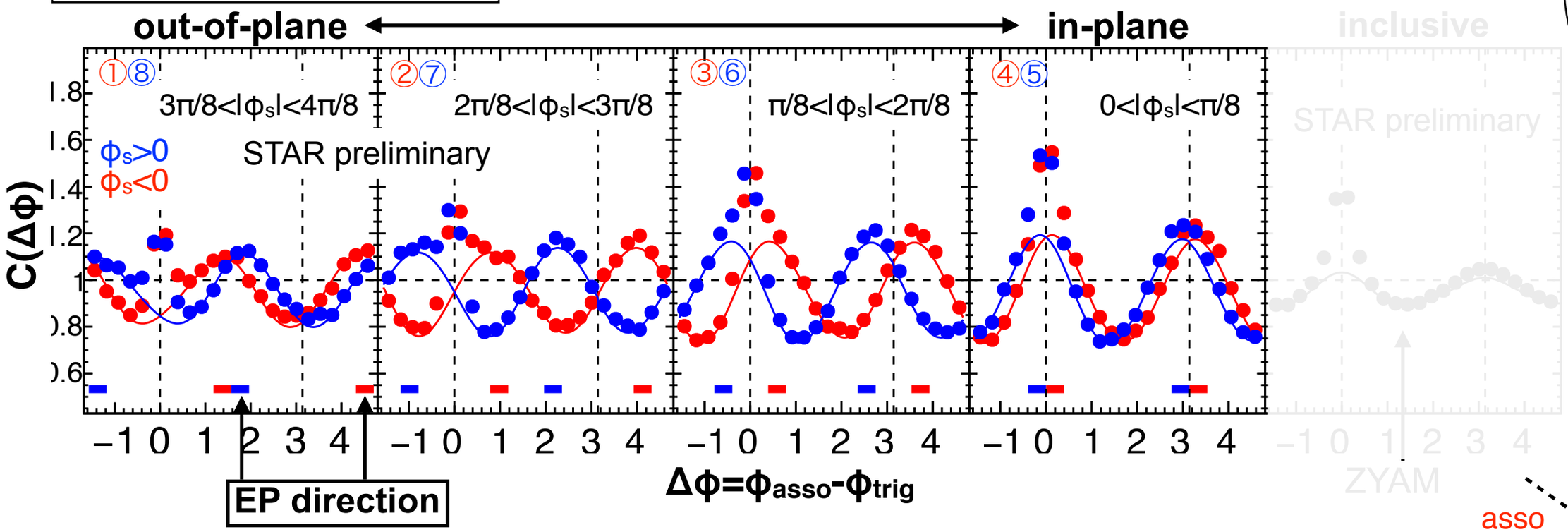

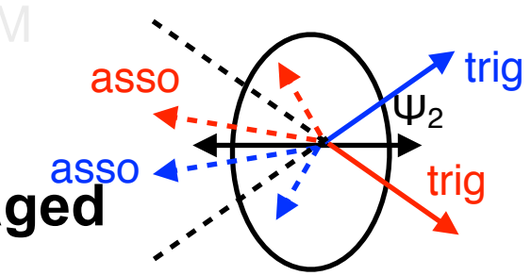

✦ Correlation shape

- Left/Right mirror symmetric trigger selection w.r.t. EP leads to **mirror-imaged distributions** on the away side

✦ Flow background subtraction

- Background **shape** is determined by data-driven simulation
- Background **level** is determined by inclusive trigger data with ZYAM assumption

✦ Correction of trigger smearing effect

- Smearing of trigger particle's angle due to limited EP resolution is corrected with unfolding method after flow subtraction

Correlations before flow subtraction and EP correction

Au+Au $\sqrt{s_{NN}}$ = 200 GeV
20-30%, w/o q_2 selection
$p_T^t \times p_T^a$=4-10x2-4 (GeV/*c*)

● raw data
— background function ($v_2 \oplus v_3 \oplus v_4$)

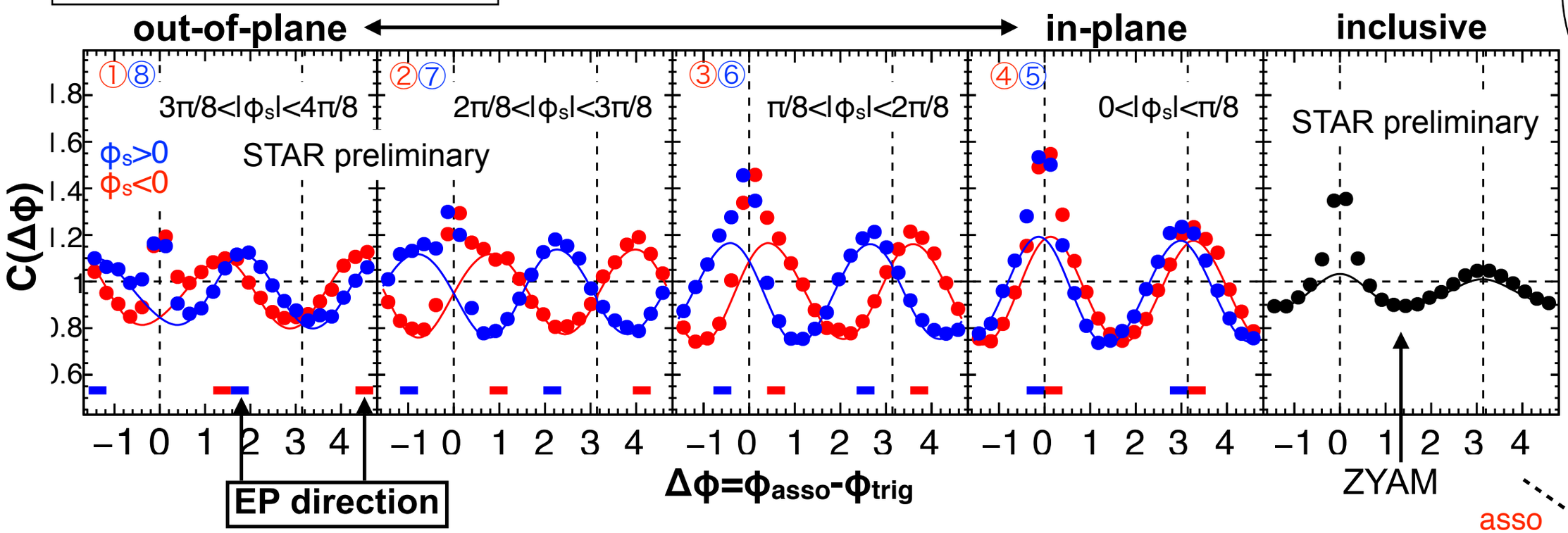

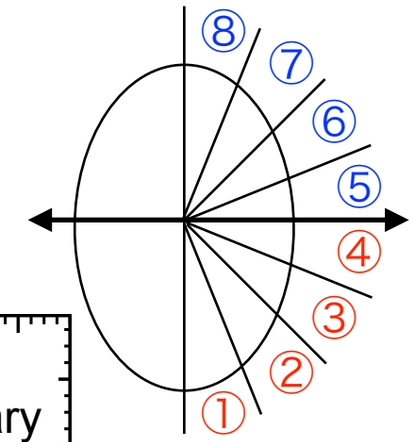

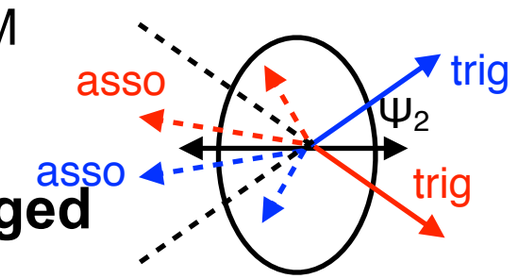

- ✦ Correlation shape
  - Left/Right mirror symmetric trigger selection w.r.t. EP leads to **mirror-imaged distributions** on the away side
- ✦ Flow background subtraction
  - Background **shape** is determined by data-driven simulation
  - Background **level** is determined by inclusive trigger data with ZYAM assumption
- ✦ Correction of trigger smearing effect
  - Smearing of trigger particle's angle due to limited EP resolution is corrected with unfolding method after flow subtraction

Correlations before flow subtraction and EP correction

Au+Au $\sqrt{s_{NN}}$ = 200 GeV
20-30%, w/o q_2 selection
$p_T^t \times p_T^a$=4-10x2-4 (GeV/*c*)

● raw data
— background function ($v_2 \oplus v_3 \oplus v_4$)

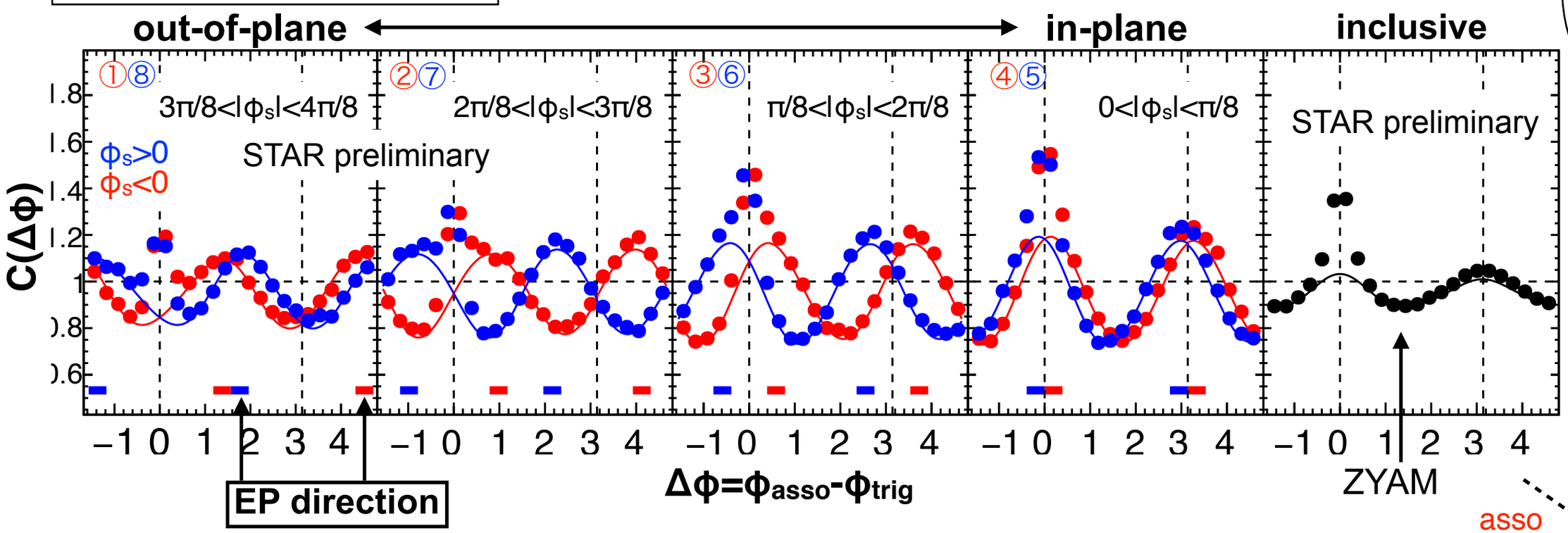

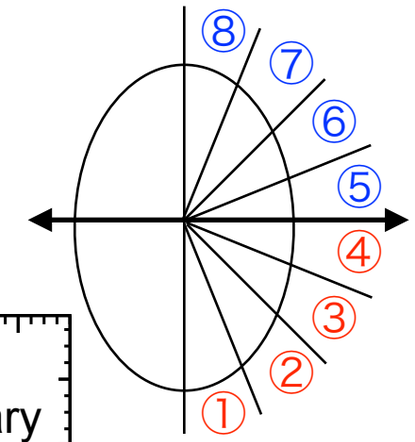

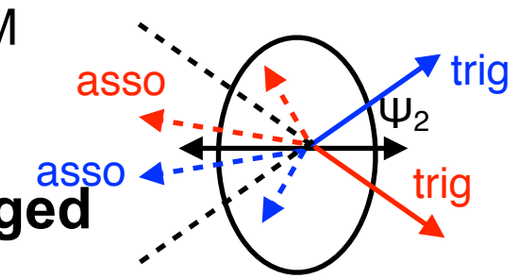

- ✦ Correlation shape
  - Left/Right mirror symmetric trigger selection w.r.t. EP leads to **mirror-imaged distributions** on the away side
- ✦ Flow background subtraction
  - Background **shape** is determined by data-driven simulation
  - Background **level** is determined by inclusive trigger data with ZYAM assumption
- ✦ Correction of trigger smearing effect
  - Smearing of trigger particle's angle due to limited EP resolution is corrected with unfolding method after flow subtraction

Correlations after flow subtraction and EP correction

Au+Au $\sqrt{s_{NN}}$ = 200 GeV
10-40%

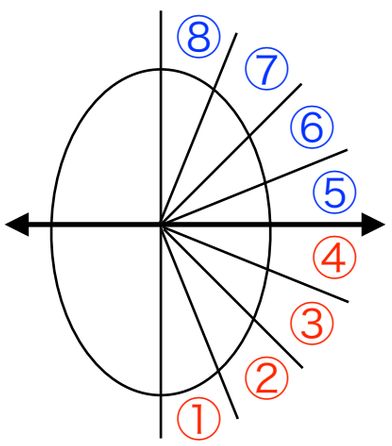

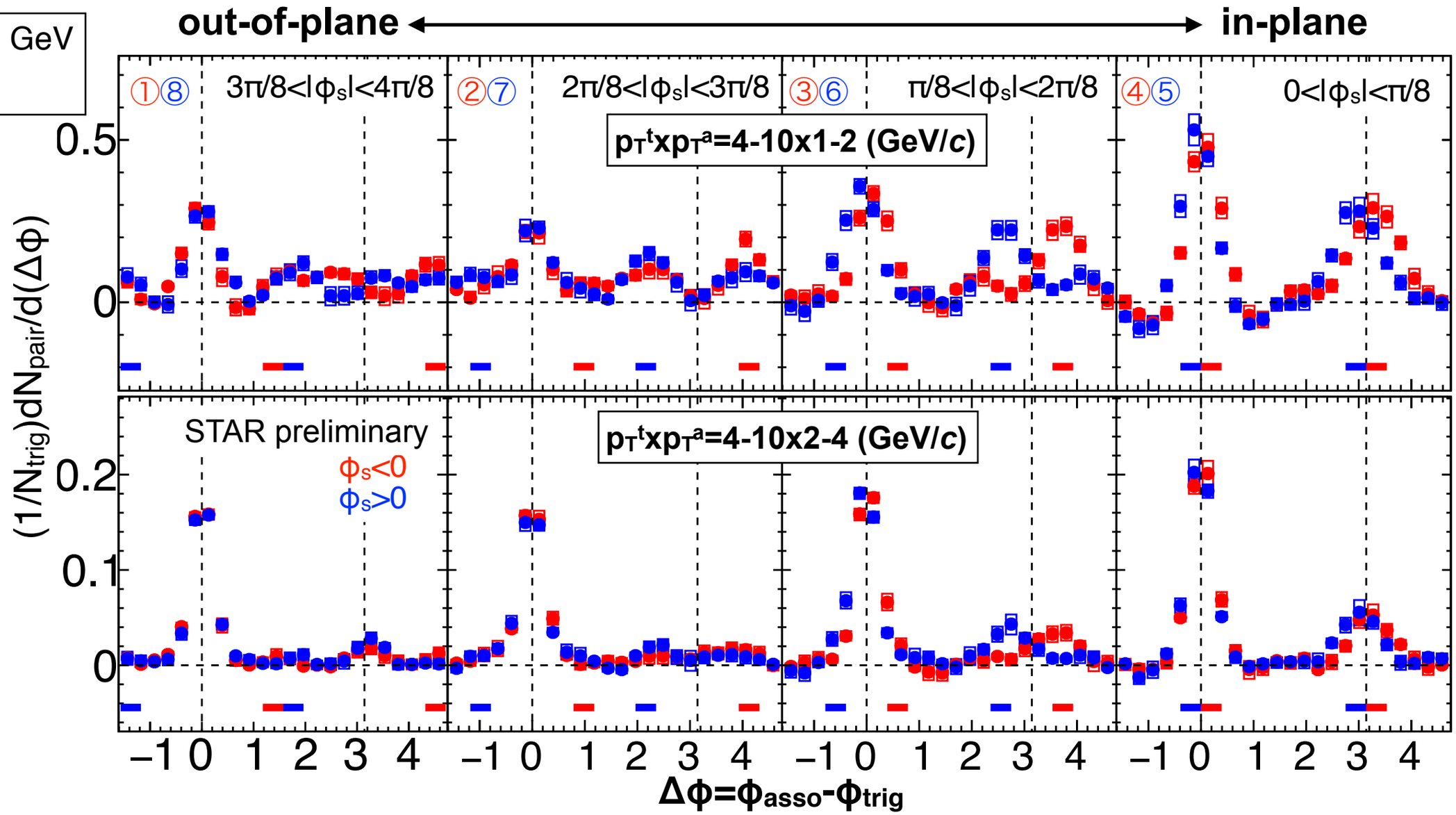

- Amplitudes increase as going to in-plane trigger on both near and away side
- Left/Right separation leads to asymmetric path length
  - averaged out in the previous measurement
- Away-side particles pushed toward in-plane direction

➡ path-length dependent jet modification

Correlations after flow subtraction and EP correction

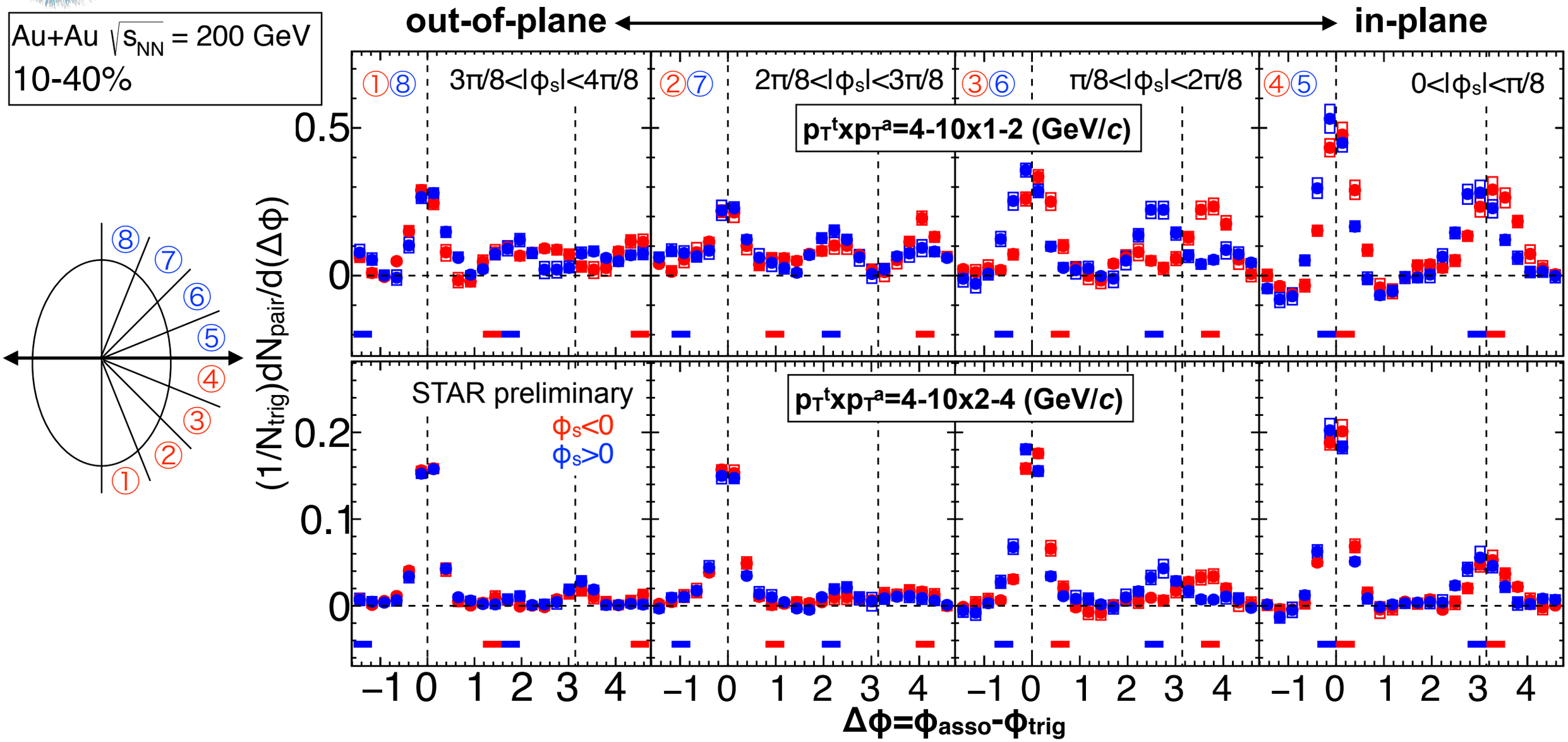

- ✦ Amplitudes increase as going to in-plane trigger on both near and away side
- ✦ Left/Right separation leads to asymmetric path length
  - averaged out in the previous measurement
- ✦ Away-side particles pushed toward in-plane direction

➡ path-length dependent jet modification

Correlations after flow subtraction and EP correction

Au+Au $\sqrt{s_{NN}}$ = 200 GeV
10-40%

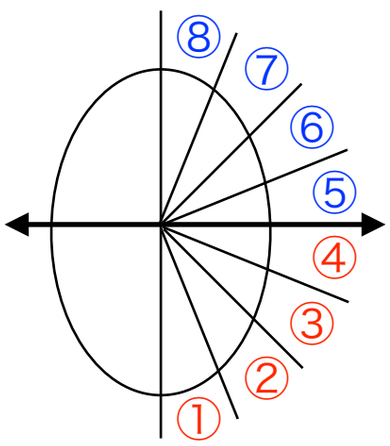

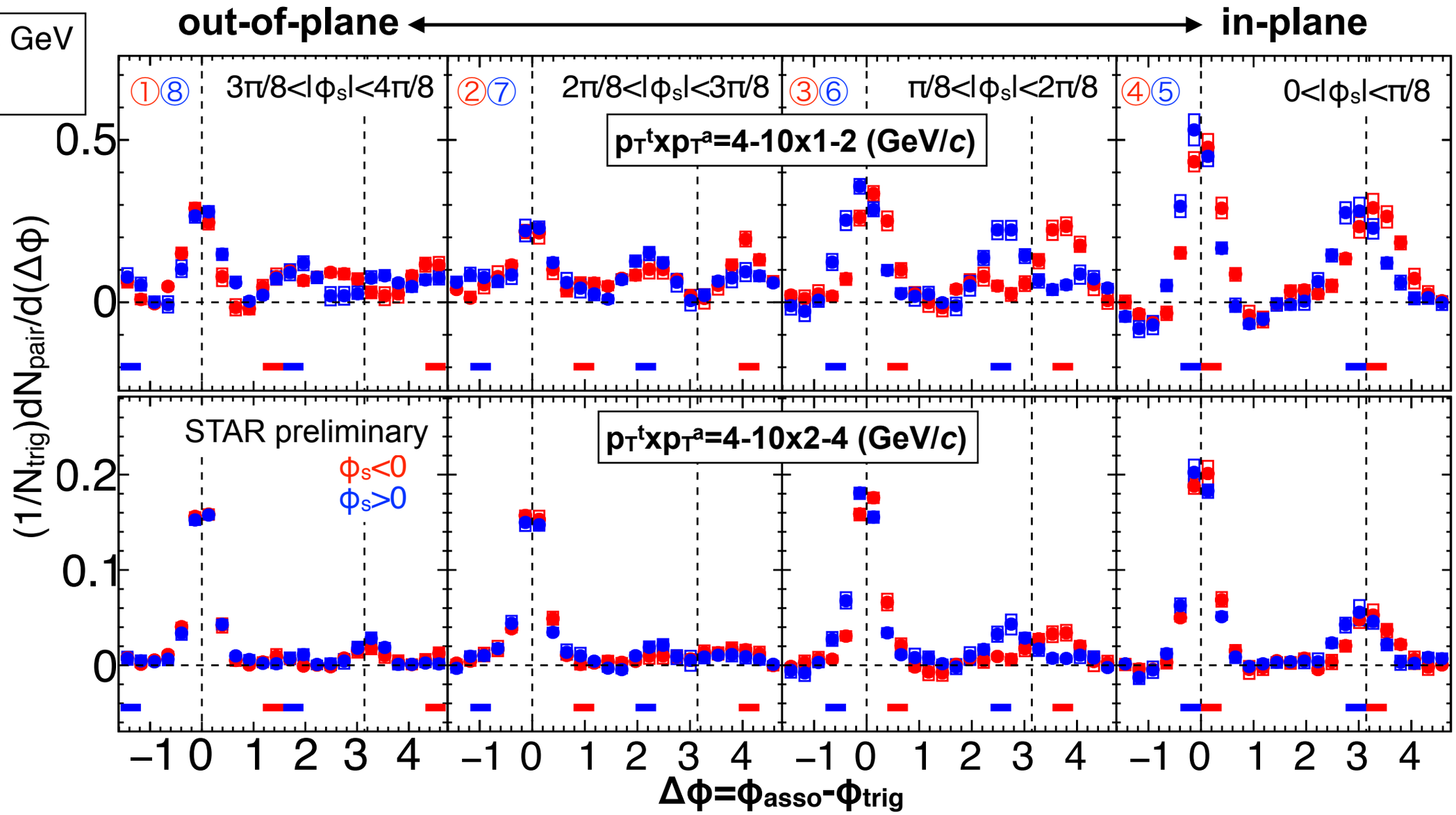

- ✦ Amplitudes increase as going to in-plane trigger on both near and away side
- ✦ Left/Right separation leads to asymmetric path length
  - averaged out in the previous measurement
- ✦ Away-side particles pushed toward in-plane direction

➡ path-length dependent jet modification

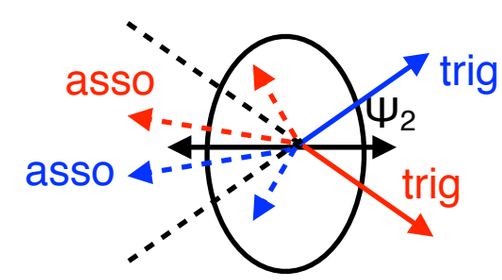

Correlations after flow subtraction and EP correction

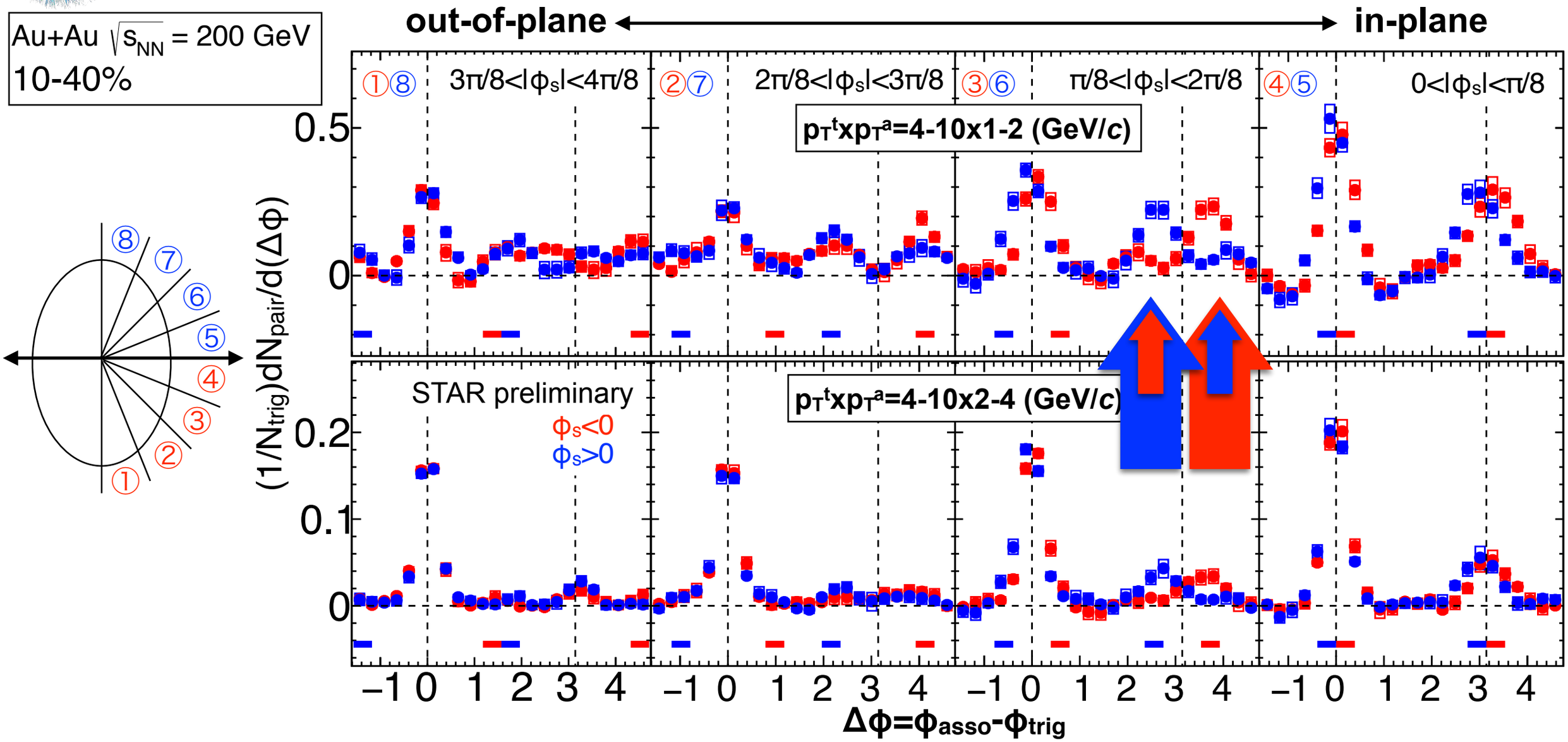

- ✦ Amplitudes increase as going to in-plane trigger on both near and away side
- ✦ Left/Right separation leads to asymmetric path length
  - ‣ averaged out in the previous measurement
- ✦ Away-side particles escaping preferentially toward in-plane direction

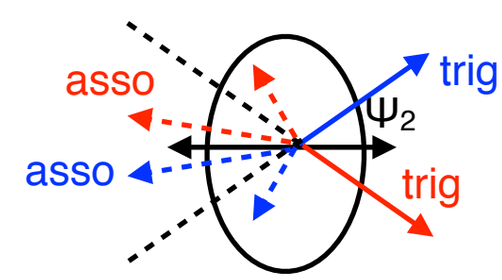

➡ path-length dependent jet modification? Role of flow?

Correlations with q_2 selection

Au+Au $\sqrt{s_{NN}}$ = 200 GeV
0-10%
- q_2 top 20%
- q_2 bottom 20%

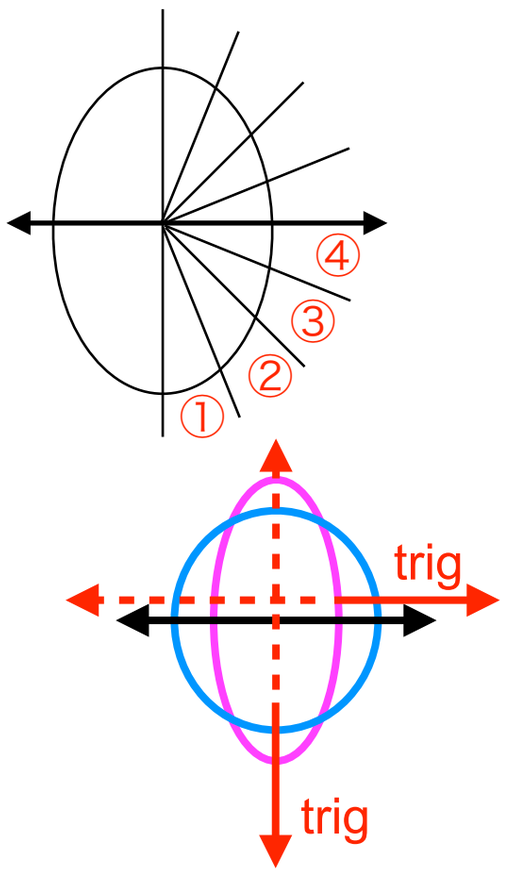

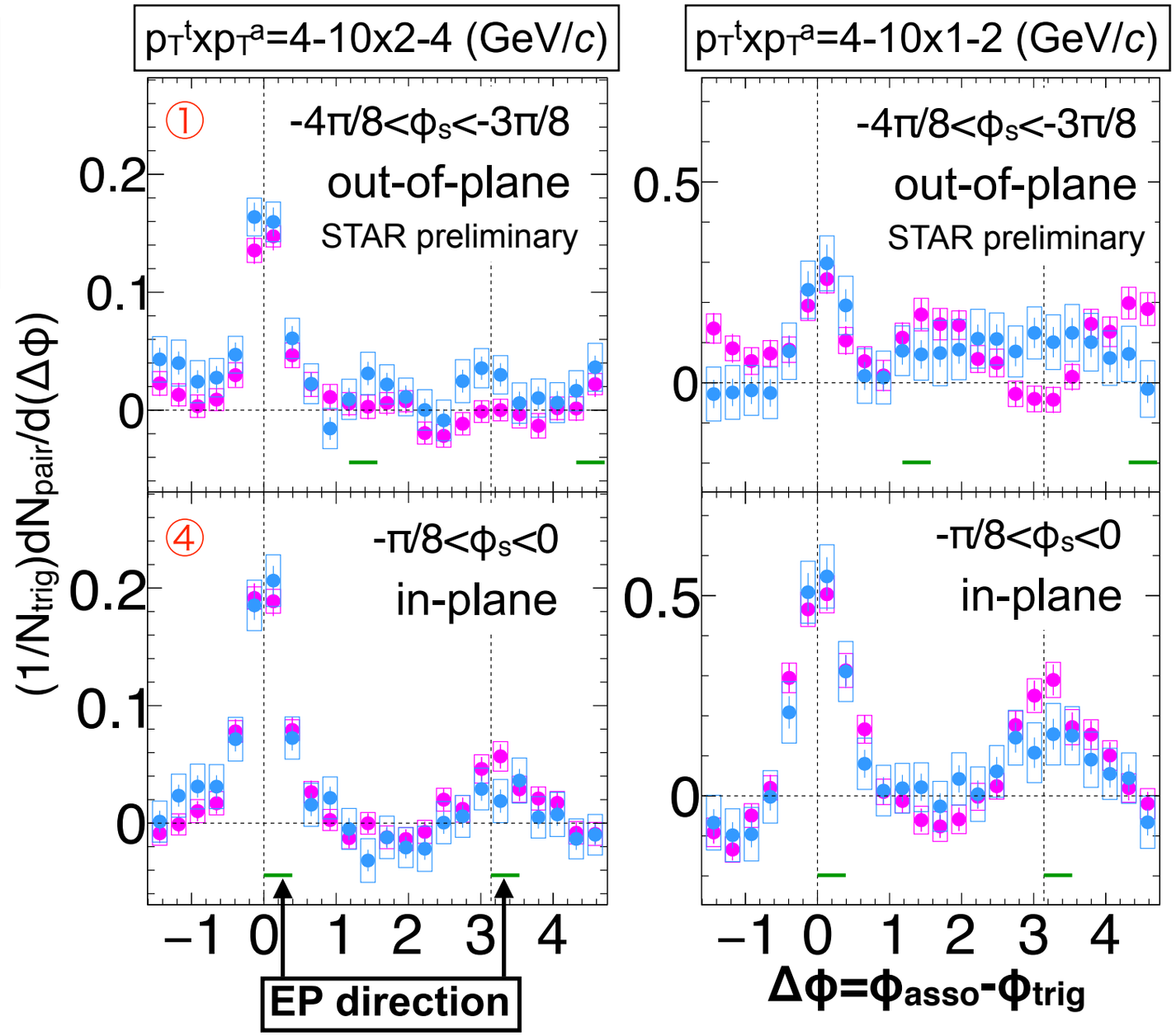

- High-p_T particles penetrate more with short path length
- Low-p_T particles are pushed toward in-plane direction and this effect is stronger in large q_2

➡ path-length dependent yield on the away side

Correlations with q_2 selection

Au+Au $\sqrt{s_{NN}}$ = 200 GeV
0-10%
- q_2 top 20%
- q_2 bottom 20%

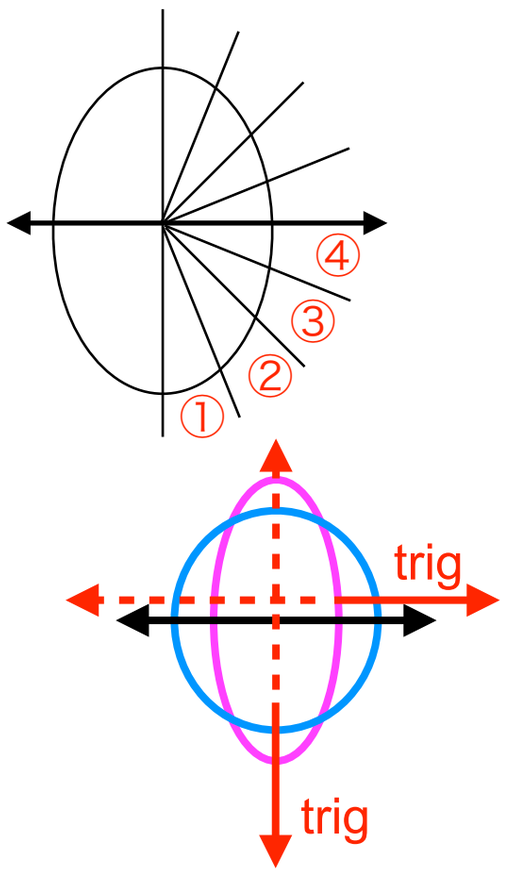

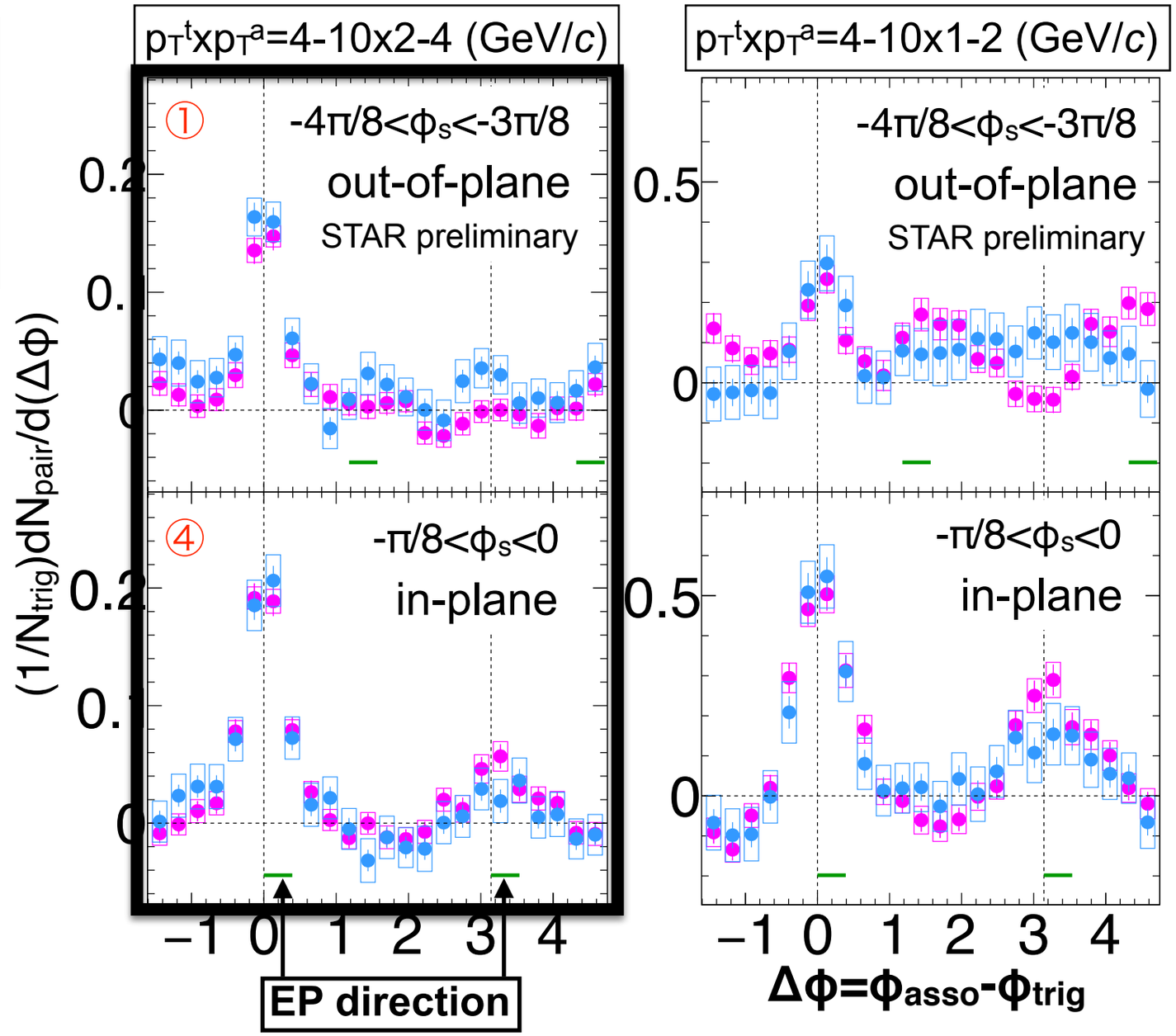

✦ High-p_T particles penetrate more with short path length

✦ Low-p_T particles are pushed toward in-plane direction and this effect is stronger in large q_2

➡ path-length dependent yield on the away side

Correlations with q_2 selection

Au+Au $\sqrt{s_{NN}}$ = 200 GeV
0-10%
- q_2 top 20%
- q_2 bottom 20%

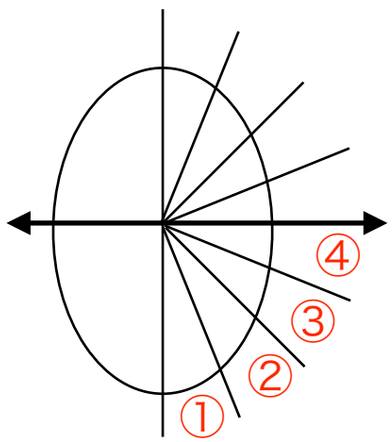

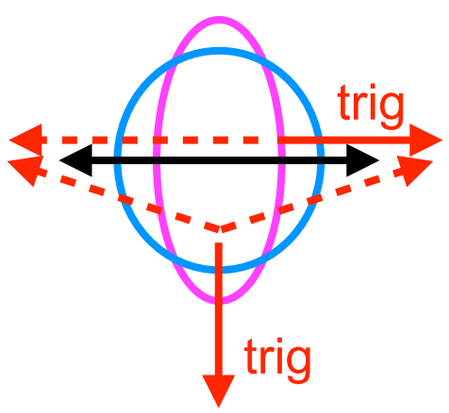

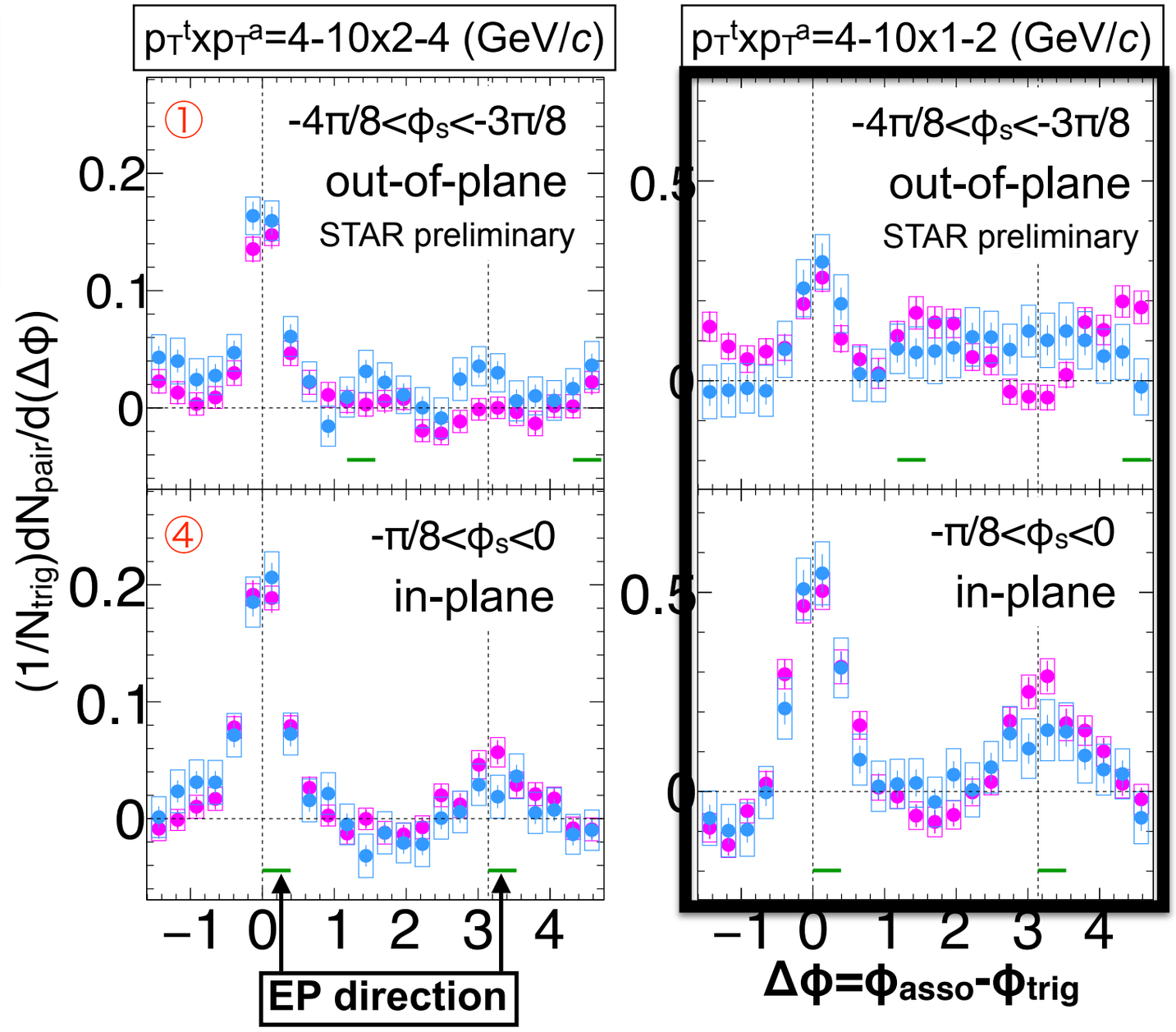

- ✦ High-p_T particles penetrate more with short path length
- ✦ Low-p_T particles are pushed toward in-plane direction and this effect is stronger in large q_2

➡ path-length dependent yield on the away side

Centrality dependence of mid-plane trigger

Au+Au $\sqrt{s_{NN}}$ = 200 GeV
$p_T^t \times p_T^a$=4-10x1-2 (GeV/*c*)
③ $-2\pi/8<\varphi_s<-\pi/8$

- q_2 top 20%
- q_2 bottom 20%

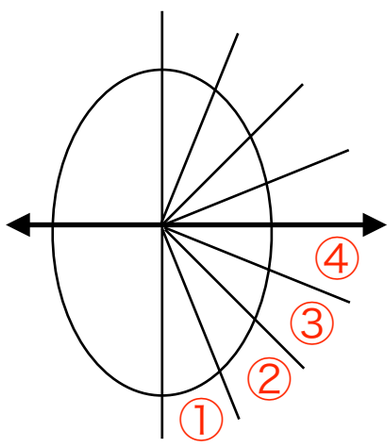

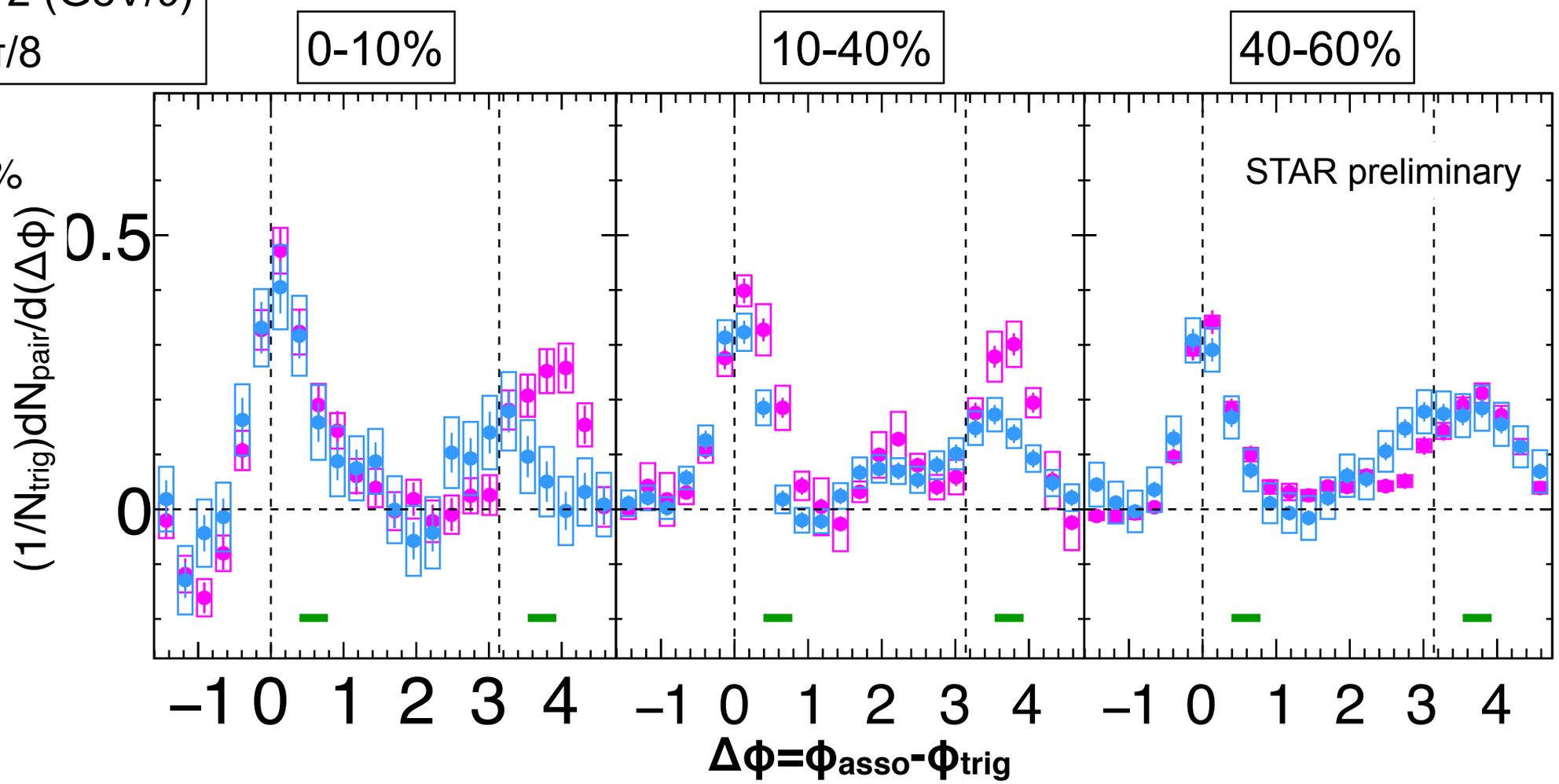

- See how shifting of away-side peak depends on centrality and q_2
- Large shift in large q_2 events
- q_2 dependence is stronger in central events
- No q_2 dependence in peripheral events

➡ Related to path-length or initial eccentricity?

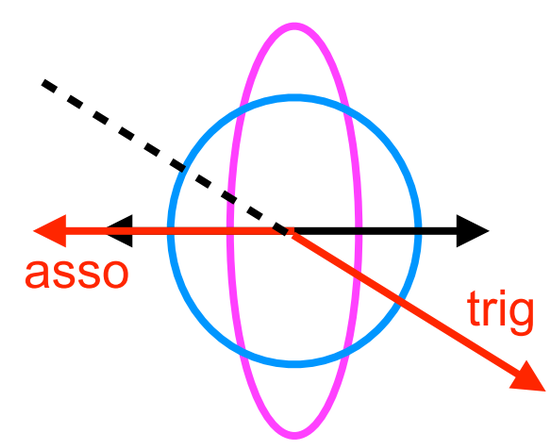

Centrality dependence of mid-plane trigger

Au+Au $\sqrt{s_{NN}}$ = 200 GeV
$p_T^t \times p_T^a$=4-10x1-2 (GeV/*c*)
③ $-2\pi/8<\varphi_s<-\pi/8$

- q_2 top 20%
- q_2 bottom 20%

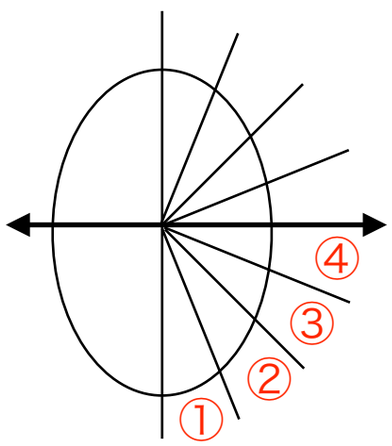

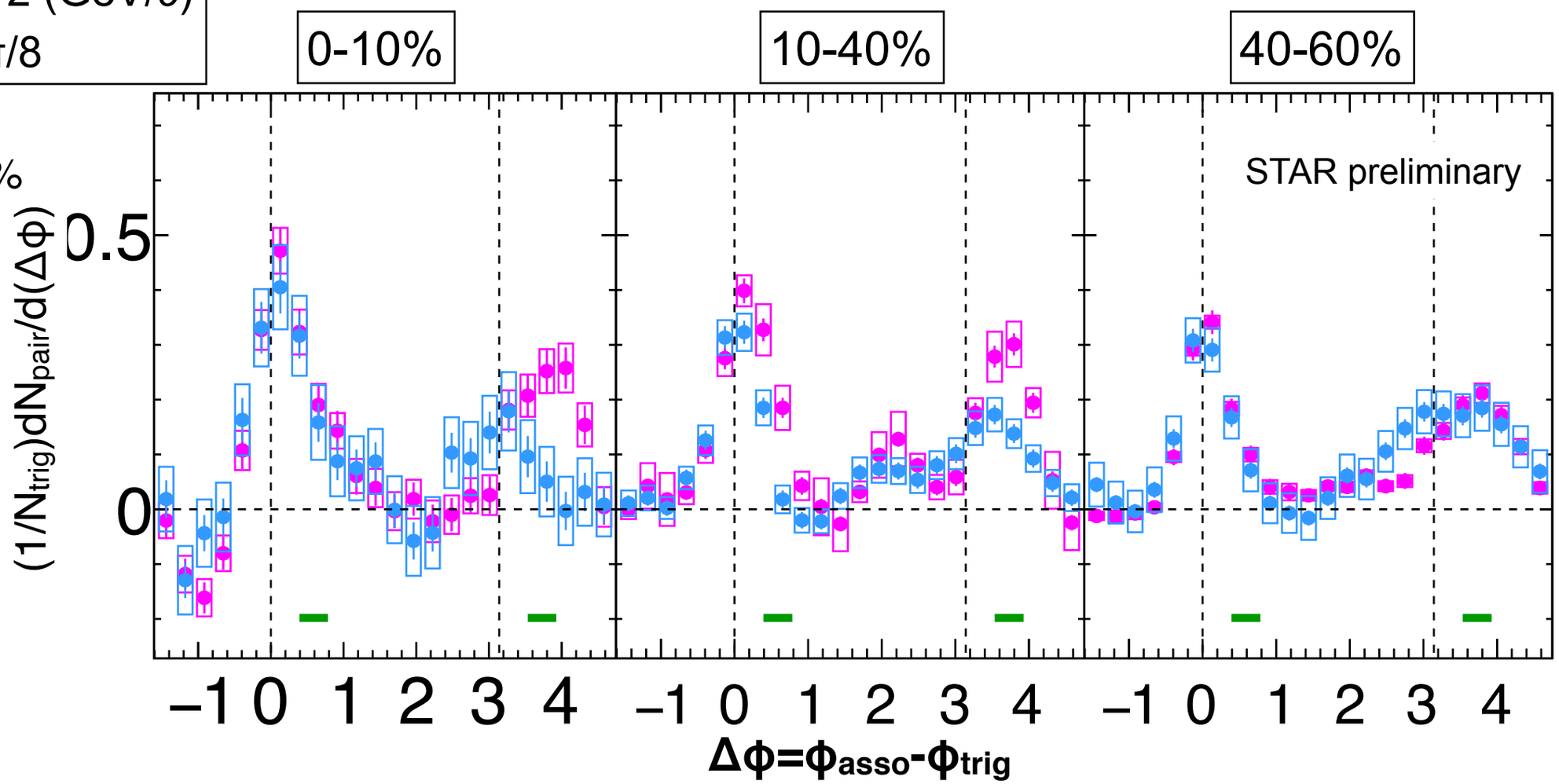

- ✦ See how shifting of away-side peak depends on centrality and q_2
- ✦ Large shift in large q_2 events
- ✦ q_2 dependence is stronger in central events
- ✦ No q_2 dependence in peripheral events

➡ Related to path-length or initial eccentricity?

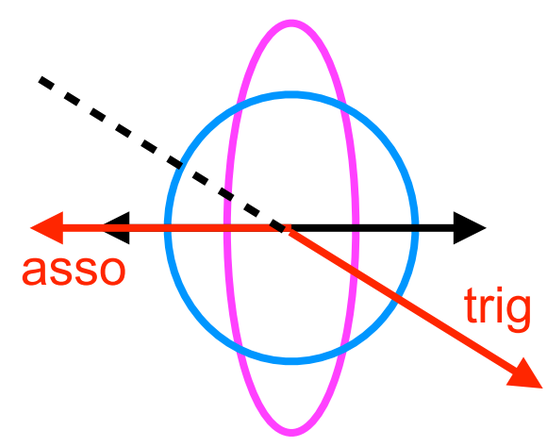

Centrality dependence of mid-plane trigger

Au+Au $\sqrt{s_{NN}}$ = 200 GeV
$p_T^t \times p_T^a$=4-10x1-2 (GeV/*c*)
③ $-2\pi/8<\varphi_s<-\pi/8$

- q_2 top 20%
- q_2 bottom 20%

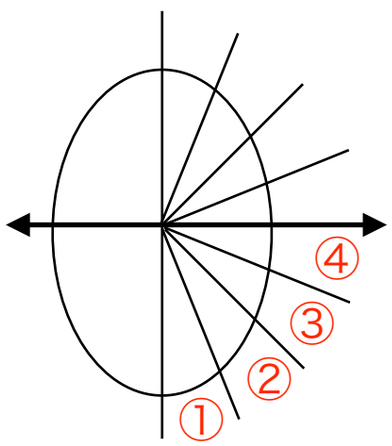

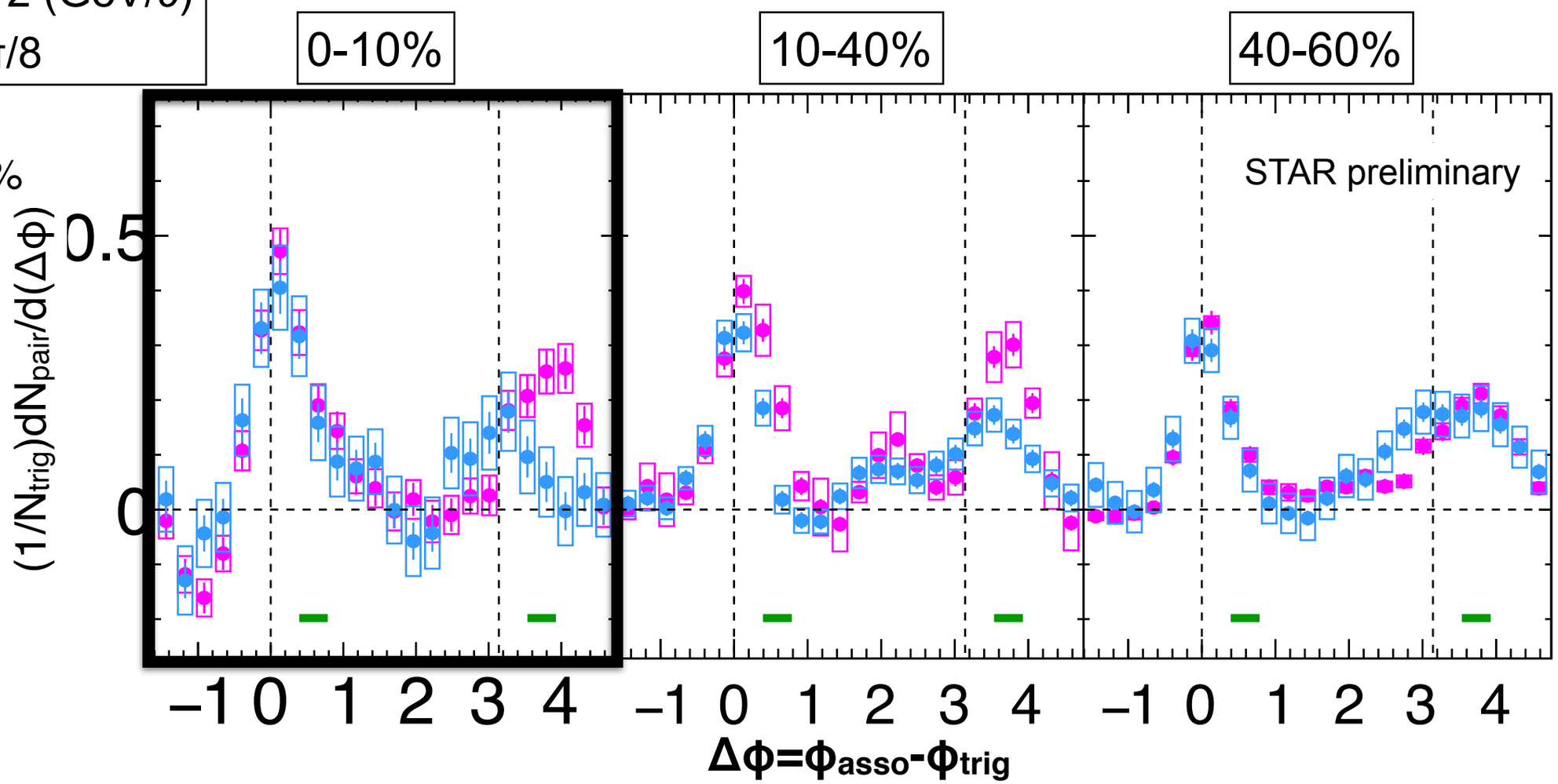

- ✦ See how shifting of away-side peak depends on centrality and q_2
- ✦ Large shift in large q_2 events
- ✦ q_2 dependence is stronger in central events
- ✦ No q_2 dependence in peripheral events

➡ Related to path-length or initial eccentricity?

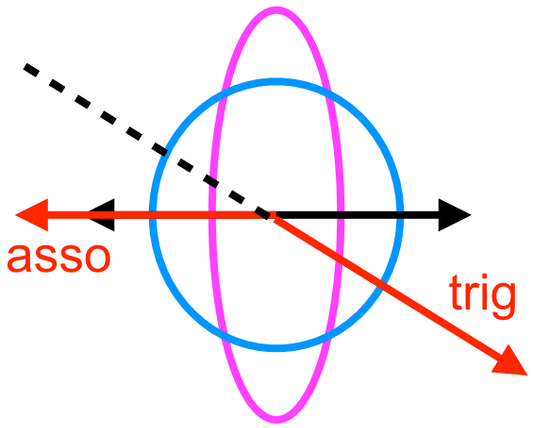

Centrality dependence of mid-plane trigger

Au+Au $\sqrt{s_{NN}}$ = 200 GeV
$p_T^t \times p_T^a$=4-10x1-2 (GeV/*c*)
③ $-2\pi/8<\varphi_s<-\pi/8$

- q_2 top 20%
- q_2 bottom 20%

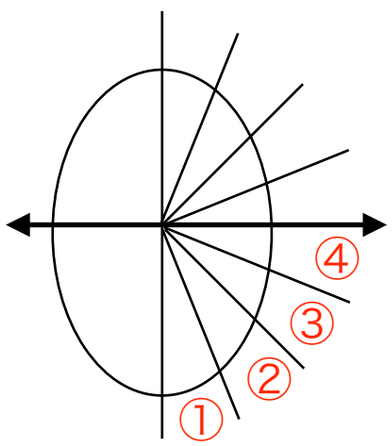

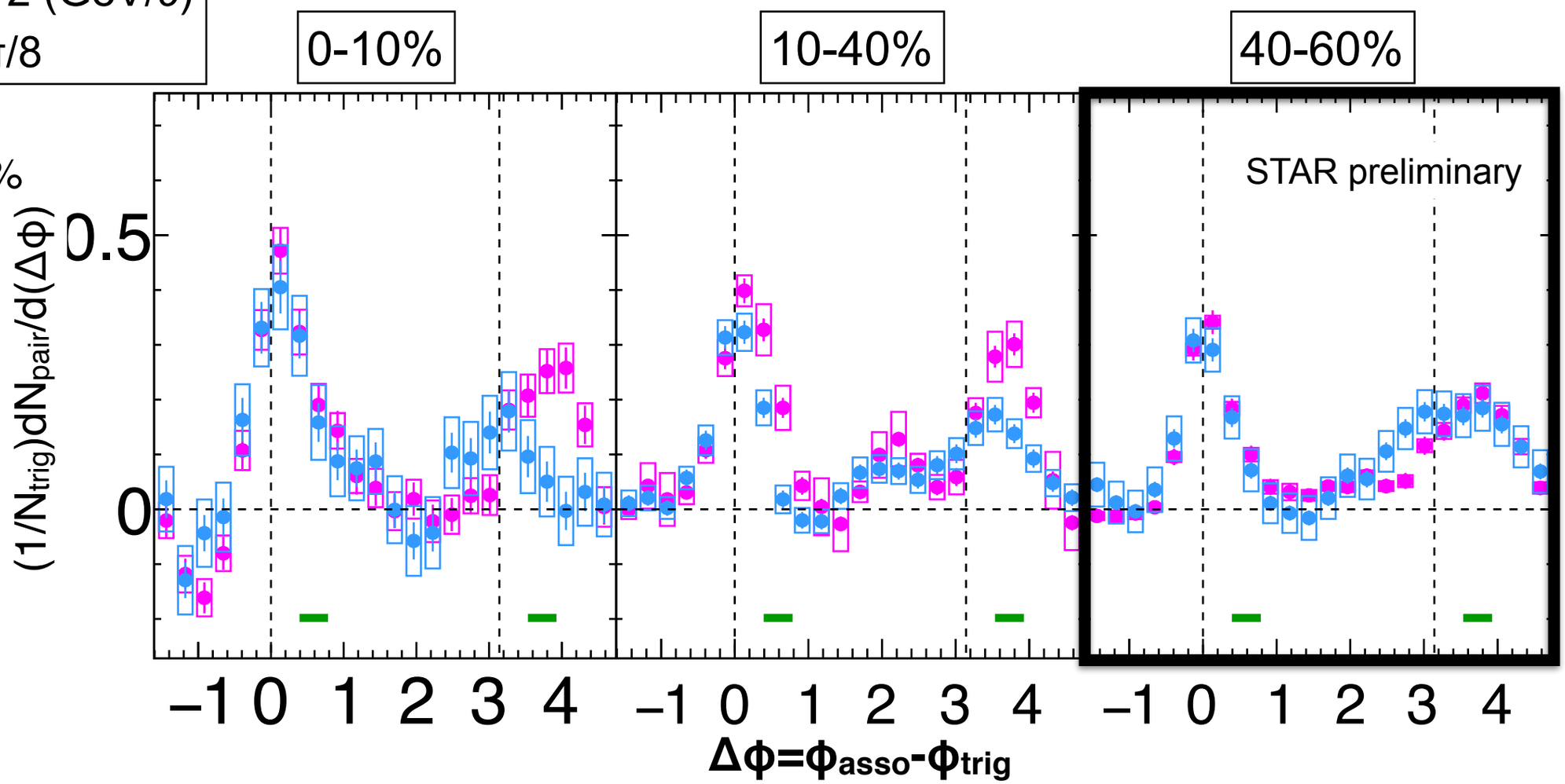

- ✦ See how shifting of away-side peak depends on centrality and q_2
- ✦ Large shift in large q_2 events
- ✦ q_2 dependence is stronger in central events
- ✦ No q_2 dependence in mid-peripheral events

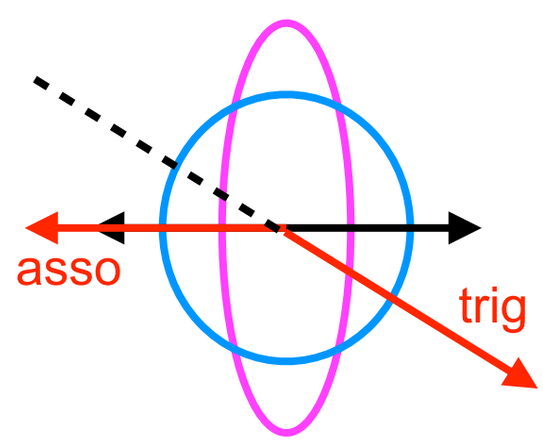

➡ Related to path-length or initial eccentricity?

Summary and outlook

Summary

- ✦ **First measurement of di-hadron correlations with respect to event plane with event shape engineering at RHIC**
- ✦ **Correlations with respect to event plane without q_2 selections**
  - Left/Right selection of trigger particles reveals path-length dependence of jet penetration
- ✦ **Correlations with respect to event plane with q_2 selections**
  - Separation between large q_2 and small q_2 events greatly enhances path-length asymmetry while preserving multiplicity
    ➡ new handle to differentially study partonic energy loss mechanisms
  - **Low p_T** particles are pushed toward in-plane direction and this effect is stronger in large q_2 events
    - Coupling with expanding medium?

Outlook

- ✦ Focus in this talk was only one p_T^{trig}, two p_T^{assc} bins
  - Much larger parameter space to be explored!
- ✦ Limitations of ZYAM assumption under investigation

Back up

Resolution of EP

Au+Au $\sqrt{s_{NN}}$ = 200 GeV

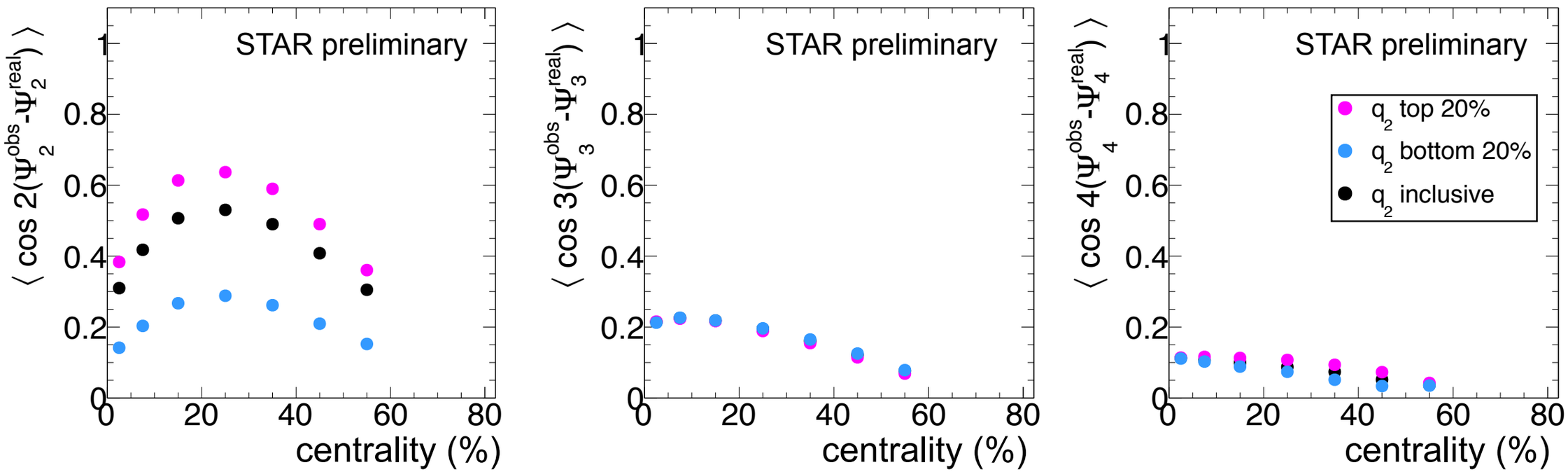

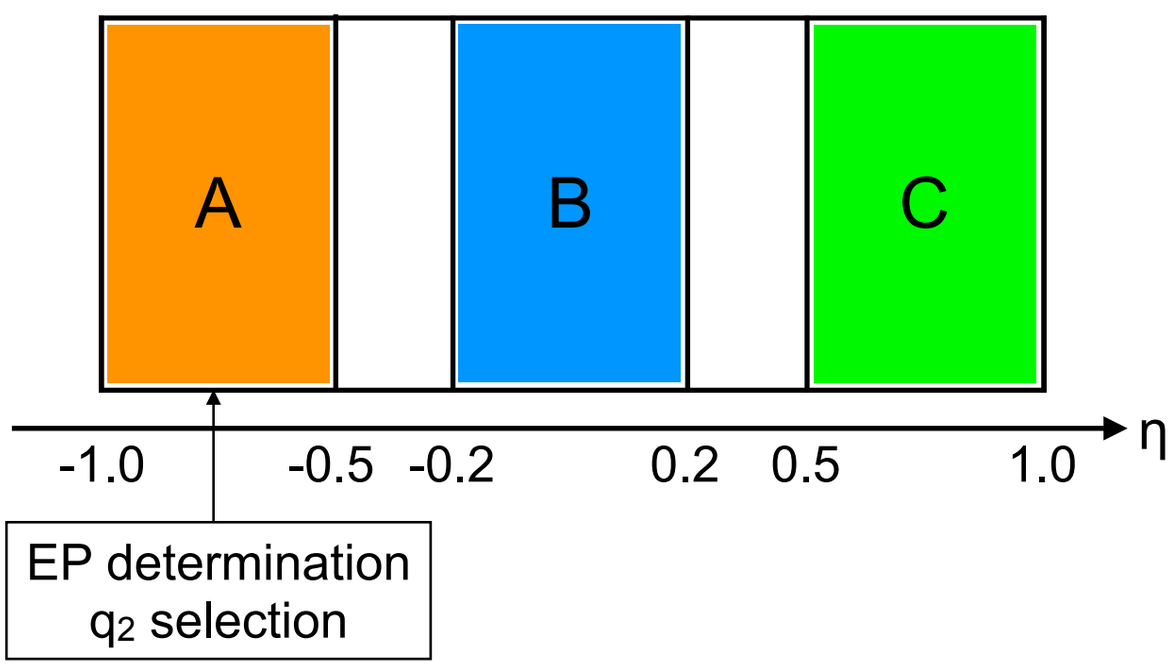

EP resolution via 3 sub-event method

$$\mathrm{Res}\{\Psi_n^A\} = \sqrt{\frac{\langle \cos n(\Psi_n^A - \Psi_n^B)\rangle \langle \cos n(\Psi_n^A - \Psi_n^C)\rangle}{\langle \cos n(\Psi_n^B - \Psi_n^C)\rangle}}$$

$\mathrm{Res}\{\Psi_n^A\}$ is shown in the upper figure

Data-driven flow MC simulation

Reconstruct flow distribution by Monte Carlo simulation

Input parameter : v_2, v_3, v_4, χ_{42}, and Res{Ψ_2}

1. generate Ψ_2, Ψ_3 at random and Ψ_4 with considering correlation between Ψ_2 and Ψ_4
2. make flow distribution which reproduce v_n
3. smear trigger particle's angle with probability distribution when selecting trigger particles angle
4. generate particles at random along the flow distribution and calculate $\Delta\phi$

Probability distribution can be written with χ_n which is calculated with following formula :

$$\left\langle \cos[kn(\Psi_n^{obs} - \Psi_n^{real})] \right\rangle = \frac{\sqrt{\pi}}{2\sqrt{2}} \chi_n e^{-\chi_n^2/4} \left[I_{(k-1)/2}\left(\frac{\chi_n^2}{4}\right) + I_{(k-1)/2}\left(\frac{\chi_n^2}{4}\right) \right]$$

Jean-Yves OLLITRAULT, PRD 48 (1993) 1132

example of probability distributions of $\Delta\Psi_2$

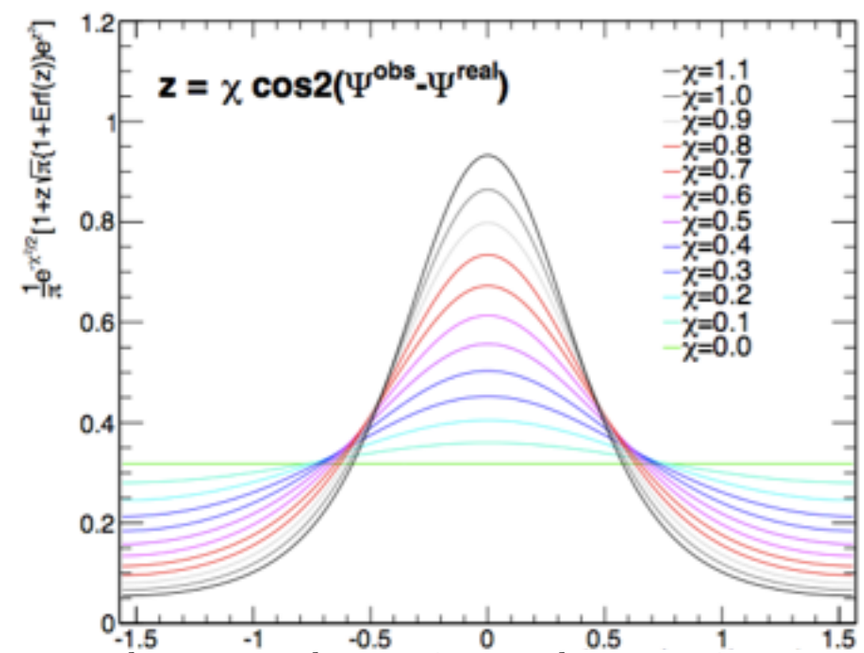

$$\Psi_n^{obs} - \Psi_n^{real} = (\phi^t - \Psi_n^{obs}) - (\phi^t - \Psi_n^{real})$$

Trigger smearing correction via fitting method

Assuming the associate-particles yield are distributed with respect to the event plane, we can correct the effect of trigger smearing due to the limited event-plane resolution which is similar to the resolution correction in the flow measurement of the single particles.

$$\frac{dN^{1+PTY}}{d(\phi^a - \Psi_2)} = 1 + Y(\phi_s, \Delta\phi)$$
$$= 1 + 2v_2^Y \cos 2(\phi_s + \Delta\phi) + 2v_4^Y \cos 4(\phi_s + \Delta\phi) \quad \text{...(1)}$$

$$\phi_s + \Delta\phi = (\phi^t - \Psi_2) + (\phi^a - \phi^t)$$
$$= \phi^a - \Psi_2$$

Applying a Fourier fitting eq.(3) to $1+Y(\varphi_s,\Delta\varphi)$ as a function of φ_s with a phase shift $\Delta\varphi$, v_n^Y can be determined and the azimuthal distributions can be corrected with corrected v_n^Y by the event-plane resolution eq.(5).

$$\frac{dN_{cor}^{1+PTY}}{d(\phi^a - \Psi_2)} = 1 + 2\frac{v_2^Y}{\sigma_2} \cos 2(\phi_s + \Delta\phi) + 2\frac{v_4^Y}{\sigma_{42}} \cos 4(\phi_s + \Delta\phi) \quad \text{...(2)}$$

$$F(\phi_s)^{raw} = 1 + 2v_2^{raw} \cos 2(\phi_s + \Delta\phi) + 2v_4^{raw} \cos 4(\phi_s + \Delta\phi) \quad \text{...(3)}$$

$$F(\phi_s)^{cor} = 1 + 2\frac{v_2^{raw}}{\sigma_2} \cos 2(\phi_s + \Delta\phi) + 2\frac{v_4^{raw}}{\sigma_{42}} \cos 4(\phi_s + \Delta\phi) \quad \text{...(4)}$$

$$1 + Y^{cor}(\phi_s, \Delta\phi) = \frac{F(\phi_s)^{cor}}{F(\phi_s)^{raw}} \cdot (1 + Y^{raw}(\phi_s, \Delta\phi)) \quad \text{...(5)}$$

$\sigma_2 = \langle \cos 2(\Psi_2^{obs} - \Psi_2^{real}) \rangle$
$\sigma_{42} = \langle \cos 4(\Psi_2^{obs} - \Psi_2^{real}) \rangle$

PHENIX, PRC 84 (2011) 024904

Trigger smearing correction via iteration method

bin-by-bin iterative unfolding correction method for $Y(\Delta\varphi,\varphi_s)$

Y^{raw} : yield before correction
O : offset
$A^{(n)}$: n-th corrected data
$B^{(n)}$: n-th smeared correlation
$C^{(n)}$: n-th correction function
x,y : index of $\Delta\varphi$ and φ_s
Y^{corr} : yield after correction

input
(raw data) + offset

$A^{(0)} = Y^{raw}+O$

smear (n-1)-th corrected data
for φ_s direction
with using probability distribution (P.21)

$B^{(n)} = SA^{(n-1)}$

make correction function
((n-1)-th corrected data) / (n-th smeared data)

$C^{(n)}(x,y) = A^{(n-1)}(x,y)/B^{(n)}(x,y)$

iteration

smooth correction function
with neighboring bins
with using smoothing parameter

$C^{(n)}(x,y) = p_{\Delta\varphi}\{C^{(n)}(x-1,y)+C^{(n)}(x+1,y)\}$
$+p_{\varphi s}\{C^{(n)}(x,y-1)+C^{(n)}(x,y+1)\}$

correction of raw data
with n-th correction function

$A^{(n)}(x,y) = C^{(n)}(x,y)*A^{(0)}(x,y)$

after converge

output
(corrected data) - offset

$Y^{corr} = A^{(n)}-O$

Sources of systematics

- ✦ v_2, v_3 and v_4
  - including track cut, EP selection, and difference between $v_n\{EP\}$ and $v_n\{2PC\}$
- ✦ EP resolution
  - difference between East and West for trigger smearing in toy-MC
- ✦ EP correlation between different order harmonics
  - only Ψ_2-Ψ_4 correlations
- ✦ ZYAM
  - $\pi/6$ (default), $\pi/12$, $\pi/4$
- ✦ Trigger smearing correction
  - range of fitting method and iteration method
  - RMS of various smoothing parameter for ϕ_s and $\Delta\phi$